

Recoloring Algorithms for Colorblind People: A Survey

MADALENA RIBEIRO, Instituto Politécnico de Castelo Branco, Portugal

ABEL J. P. GOMES, Instituto de Telecomunicações and Universidade da Beira Interior, Portugal

Color is a powerful communication component, not only as part of the message meaning but also as a way of discriminating contents therein. However, 5% of the world's population suffers from color vision deficiency (CVD), commonly known as colorblindness. This handicap adulterates the way the color is perceived, compromising the reading and understanding of the message contents. This issue becomes even more pertinent due to the increasing availability of multimedia contents in computational environments (e.g., web browsers). Aware of this problem, a significant number of CVD research works came up in the literature in the past two decades to improve color perception in text documents, still images, video, and so forth. This survey mainly addresses recoloring algorithms toward still images for colorblind people, including the current trends in the field of color adaptation.

CCS Concepts: • Human-centered computing → Accessibility systems and tools; • Computing methodologies → Image processing; Perception;

Additional Key Words and Phrases: Color vision deficiency, color blindness, color perception

ACM Reference format:

Madalena Ribeiro and Abel J. P. Gomes. 2019. Recoloring Algorithms for Colorblind People: A Survey. *ACM Comput. Surv.* 52, 4, Article 72 (August 2019), 37 pages.

<https://doi.org/10.1145/3329118>

1 INTRODUCTION

Color is a powerful feature that eases communication among humans. Color is present in many aspects of our daily lives. Children use crayons to express themselves through forms and colorful scribbles. Color is a part of many things of everyday life, including the food we eat, the natural and urban landscapes where we live, and the clothes we wear. We can even say that, in some sense, color reflects the personality of each person (the style, culture, and even age).

Nevertheless, about 5% of the world's population suffers from a handicap called *color vision deficiency* (CVD), commonly known as *colorblindness*, though the rate of incidence for men is 8% [39]. Fortunately, the higher rates of incidence occur in less severe types (i.e., anomalous trichromats and dichromats). CVD has different types and degrees of severity depending on the type and the number of affected photoreceptor cells of the eye. This impairment impedes, limits, or distorts the perception of color, sometimes reducing the gamut of visible colors, interfering with the

This research has been partially supported by the Portuguese Research Council (Fundação para a Ciência e Tecnologia), under the FCT Project UID/EEA/50008/2019.

Authors' addresses: M. Ribeiro, Instituto Politécnico de Castelo Branco, ESART, 6000-767 Castelo Branco, Portugal; email: mribeiro@ipcb.pt; A. J. P. Gomes, Universidade da Beira Interior, Departamento de Informática, 6200-001 Covilhã, Portugal; email: agomes@di.ubi.pt.

Permission to make digital or hard copies of all or part of this work for personal or classroom use is granted without fee provided that copies are not made or distributed for profit or commercial advantage and that copies bear this notice and the full citation on the first page. Copyrights for components of this work owned by others than ACM must be honored. Abstracting with credit is permitted. To copy otherwise, or republish, to post on servers or to redistribute to lists, requires prior specific permission and/or a fee. Request permissions from permissions@acm.org.

© 2019 Association for Computing Machinery.

0360-0300/2019/08-ART72 \$15.00

<https://doi.org/10.1145/3329118>

interpretation of images and generic documents, and, consequently, the communication and interaction process between humans (i.e., it may provoke bias on the message, no matter it is implicit or explicit).

In this context, and for the first time, we put forward a survey of color adaptation algorithms for CVD people, with a focus on still images, yet they also apply to other media like text and video. Our methodology addresses the ability of color adaptation methods in preserving the *perceptual learning* of CVD people as much as possible. For example, a deutanope-type dichromat person sees an orange in faded green, so it is not a good idea to re-color it in blue, because his/her perceptual experience tell him/her that an orange is not a blue piece of fruit. So, the following perceptual requirements must be satisfied to preserve the perceptual learning:

- **Color naturalness.** Preserving color naturalness means minimizing the perceptual difference between an original color and the color after adaptation. This requirement allows us to not break up with the perceptual learning of the colorblind.
- **Color consistency.** Preserving color consistency means that a given color is always remapped to the same color, independently of the set of colors subject to remapping. Otherwise, we cannot avoid some disorientation in the perception of the colorblind.
- **Color contrast.** In the process of color adaptation, preserving or enhancing color contrast is essential to be able to distinguish adjacent objects in a given image. Sometimes, it is even necessary to identify objects seen as a single object by a CVD person.

The critical analysis of the recoloring methods surveyed in this article builds upon those three perceptual requirements. Besides, this survey organizes itself as follows. Section 2 introduces color perception and color vision deficiency. Sections 3, 4, and 5 describe and compare recoloring algorithms for anomalous trichromats, dichromats, and monochromats, respectively. Section 6 carries out a critical analysis of the state-of-the-art recoloring methods, their current trends, and challenges, as well as some hints for future work. Section 7 draws the most relevant conclusions of our study.

2 COLOR PERCEPTION

Color perception involves the eye and nervous system. In the human eye, there are photosensitive cells in the retina, called cones. They receive the stimulus from light, transducing it into chemical signals. Then, neurological structures conduct such signals to the brain [52]. There are three types of cones: S-cones (blue-cones), which are light sensitive to small wavelengths; M-cones (green-cones), which are sensitive to medium wavelengths; and L-cones (red-cones), which are sensitive to long wavelengths [78]. According to the so-called tristimulus theory [52, 78], the perception of color results from blending those three signals of distinct wavelengths into a single signal. When human color perception works well by combining small, medium, and long wavelength signals, we are in the presence of a *color-normal trichromat person* (or merely a *trichromat*) who perceives all colors of the visible spectrum, yet he/she is only capable of distinguishing about 700 different tones [73].

However, not all people perceive color as a trichromat individual. Color vision deficiency (CVD), also known as colorblindness or daltonism, can be acquired by way of cortical trauma [15, 75], brain fever [58], disorders, degenerations, dystrophy or diseases of different origin, diabetes *mellitus*, and exposure to toxic agents [5]. Nevertheless, the most common CVD type originates in genetic alterations of cone cells (opsins) [78]. Depending on the number of affected color channels, we can classify CVD into three main categories [4, 78], as shown in Figure 1.

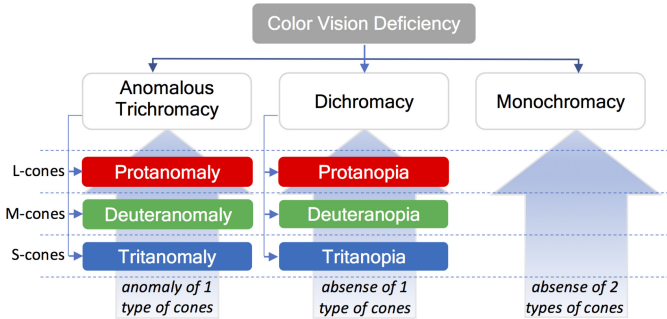


Fig. 1. Taxonomy of color vision deficiencies.



Fig. 2. Color gamuts when seen by (a) color-normal trichromats and ((b), (c), and (d)) anomalous trichromats using the simulation algorithm in Reference [50] with a severity degree of 0.5.

- **Anomalous trichromacy.** In this case, the curve of the sensitivity of one type of cone cells shifts from its regular position, which distorts color perception, although the color gamut is mostly the same as for people without CVD.
- **Dichromacy.** The color space of a dichromat individual is two dimensional (2D), because he/she only owns cones of two types, that is, cones of the third type are missing or do not function at all; consequently, his/her perceived color spectrum substantially is reduced.
- **Monochromacy.** In this case, two or even three types of cones are missing or do not work at all. Consequently, color vision relies on rods, which allow for grayscale vision. That is, the color space of a monochromat individual is 1D.

Depending on the type of malfunctioning cones, there are three *anomalous trichromacy types*, namely protanomaly (protan), deutanomaly (deutan), or tritanomaly (tritan), which are related to the sensitivity loss of either L-, M-, or S-cones, respectively [78]. Furthermore, the anomalous trichromacy has a degree of severity, which varies from 0.1 to 0.9 [93]. Figure 2 illustrates how the low-severity anomalous trichromats see. The loss of sensitivity of one type of cones means that colors look less vivid for anomalous trichromats; for example, both protanomalous and deutanomalous people see reddish hues as rusty and close to browns, while tritanomalous people see bright yellows, as well as blues and greens, as dull colors.

There are also three *dichromacy types*, namely protanopia (protan), deutanopia (deutan), and tritanopia (tritan), which refer to the absence of L-, M-, or S-cone cells, respectively, on the retina [78]. Protanopes and deutanopes have difficulties in distinguishing between red and green colors; hence, the so-called red/green colorblindness. Tritanopes do not distinguish blues from greens and yellows from magentas [8, 78]. Figure 3 shows how dichromats perceive colors. Their color gamut is quite limited, because the 3D color space perceived by a trichromat reduces to 2D; specifically, protanopes and deutanopes only see blues and yellows (with more or less lightness), while tritanopes merely see reds and cyans (with more or less brightness).

Fortunately, only a few people are monochromat. Monochromacy is the severest type of CVD, because two or even three types of cones do not work at all or do not exist. There are two types of monochromacy: *blue-cone monochromacy*, when only the S-cone cells are working [23], and



Fig. 3. Color gamuts when seen by (a) color-normal trichromats, ((b) and (c)) protan and deutan dichromats using the simulation algorithm in Reference [86], and (d) tritan dichromats using the simulation algorithm in Reference [66].

rod monochromacy, when the three types of cones are either missing or non-functioning for some reason. Rod monochromacy (or achromatopsia) is characterized by a total lack of color experience, as well as low visual acuity, so that rod monochromat people only see grayscale shades, as in scotopic vision [54, 78]. Concerning blue-cone monochromacy, it is characterized by a grayscale vision with some shades of blue [70].

3 CVD RECOLORING METHODS FOR ANOMALOUS TRICHROMACY

The anomalous trichromacy characterizes by the weakness of the sensitivity of a single type of cone cells, L (long-wavelength-sensitive cones), M (medium-wavelength-sensitive cones), or S (short-wavelength-sensitive cones). Anomalous trichromats see all the colors in the visible electromagnetic spectrum but in a distorted way. Regarding the base color space, the recoloring methods described below to address anomalous trichromacy divide into five categories: LMS, RGB, HSx variants, CIE variants, and YCC variants. See Reference [18] for further details about color spaces.

3.1 LMS-based Methods

We only found a relevant LMS-based method for anomalous trichromacy. It is in Yang et al. [94], following their preliminary works described in References [92] and [93]. Based on these works, Yang et al. developed an algorithm later incorporated into Digital Item Adaptation (DIA), a module of the standard MPEG-21 framework.

Yang et al.’s method [94]. Let (L, M, S) be a color as seen by a trichromat person. As known, a deutan person sees the color (L, M, S) as (L, M', S) , with $M' < M$. Note that (L, M', S) can be obtained from (L, M, S) using the matrix \mathbf{M} introduced by Brettel et al. [7, 86] to simulate the deutan color vision; similarly, one utilizes the matrices \mathbf{L} and \mathbf{S} for protanomaly and tritanomaly, respectively. Therefore, one needs to perform the color correction by increasing the value of M' toward M as much as possible. This is done by applying the inverse matrix \mathbf{M}^{-1} to (L, M, S) , not to (L, M', S) ; otherwise, the individual continues to see (L, M, S) as (L, M', S) . Thus, the recoloring pipeline $(R, G, B) \rightarrow (L, M, S) \xrightarrow{\mathbf{M}^{-1}} (L, M', S) \rightarrow (R', G', B')$ with $M' > M$ allows, in principle, a color-normal trichromat and a deutan trichromat perceive (L, M, S) and (L, M', S) , respectively, as the same color. However, this increasing color compensation may be not sufficient for values of M close to the upper bound of M , because they overlap at the upper bound of M .

Indeed, applying the inverse matrix M^{-1} to the original image leads to values of the RGB components exceeding the 255 standard value. Therefore, one needs to normalize the RGB components of each pixel, but this leads to brightness issues. Aware of this problem, You and Park [95] explored the backlight property of LCDs to optimize the normalization post step of the RGB colors to improve the final quality of images.

Analysis of perceptual metrics: Yang et al. [94] adopted a compensation strategy by increasing the values of L , M , or S for protan, deutan, and tritan trichromats, respectively. Therefore, this method enhances the image contrast, unless the pixel colors are already very vivid (i.e., they are close to color space bounds). The LMS-to-RGB matrix ensures that (L, M, S) is mapped to the same

(R, G, B) , so Yang et al.'s method is color consistent. However, increasing the value of L for protan people implies not only increasing R but also decreasing G and B (cf. LMS-to-RGB matrix) so that all pixels change their RGB colors. Consequently, color naturalness is not preserved unless the increase of L is relatively small. Indeed, increasing the value L may change blues to magentas, cyans to pinks, greens to yellows, and so forth.

3.2 RGB-based Methods

We found three RGB-based recoloring methods for anomalous trichromacy. The first is for protan trichromats (i.e., weak red vision) [67], the second applies to protan and deutan trichromats and protan and deutan dichromats [45], while the third applies to any CVD [20].

Poret et al.'s method [67]. This color compensation method is only for those with weak red vision (i.e., protan people). It builds upon the fact that protan people perceive better the dark, saturated red shades than dull, light red shades. This fact explains why they compressed the range $[0, 255]$ of reds (R channel) into $[0, 205]$, i.e., about 20% less of red value; this is valid for all colors with some amount of R . Therefore, all the pixels with some red are subject to recoloring. That is, all pixels without any red ($R = 0$) remain unchanged in the recoloring process. In terms of HSV color space, the reduction of 20% in the RGB range of reds provokes a counterclockwise rotation for hues greater than 0° and a clockwise rotation for hues less than 360° ; for example, vibrant yellow $(255, 255, 0)$ changes to a yellowish green $(205, 255, 0)$, while a lilac likely maps to a blue. In addition, if $R > G, B$, then the saturation of (R, G, B) decreases; otherwise, if R is not dominant in (R, G, B) , then its color saturation increases after the compensation process. In short, the recoloring pipeline of this method is given by the mapping $(R, G, B) \rightarrow (R', G, B)$, where $R' = R(1 - r)$, with $r = 205/255$.

Analysis of perceptual metrics: Taking into consideration that the mapping $R \rightarrow R'$ of each color is deterministic, we readily conclude that color consistency holds in the recoloring process. In addition, the method described in Reference [67] enhances color contrast, because the reds get darker and more saturated; consequently, the protan person's color perception gets better, because his or her weak red vision is compensated by using stronger (or more saturated) reds. The downside is that some pixel colors may lose naturalness; for example, a magenta may be seen as a lilac.

Lee-Santos method [45]. Unlike most recoloring methods, Lee and Santos [45] (see also Reference [44]) did not consider only extreme cases of color blindness but varying degrees of protanomaly $\alpha \in [0, 1]$ and deuteranomaly $\beta \in [0, 1]$ for anomalous trichromats; for trichromats, we have $\alpha = \beta = 0$ (no anomaly), whereas $\alpha = 1$ or $\beta = 1$ for dichromats. These CVD values are obtained by prior diagnosis. Their main contribution lies in both the unified simulation model and the unified recoloring model for anomalous trichromats (with varying degrees of severity), including color-normal trichromacy (no anomaly) and dichromacy as extreme cases. Indeed, they introduced two recoloring methods, called A and B, which essentially are compensation methods for the lack of sensitivity to specific color spectral bands. For example, the recoloring method B builds upon the pipeline $(R, G, B) \xrightarrow{M} (R', G', B')$, where

$$M = \begin{bmatrix} \left(1 - \frac{\beta}{2}\right) & \frac{\beta}{2} & 0 \\ \frac{\alpha}{2} & \left(1 - \frac{\alpha}{2}\right) & 0 \\ \frac{\alpha}{4} & \frac{\beta}{4} & 1 - \frac{\alpha+\beta}{4} \end{bmatrix}$$

denotes the unified matrix that allows for recoloring images for (protan and deutan) trichromats and (protan and deutan) dichromats characterized by (α, β) . This process is customizable for any colorblind person, except for tritan trichromats, tritan dichromats, and monochromats, which are

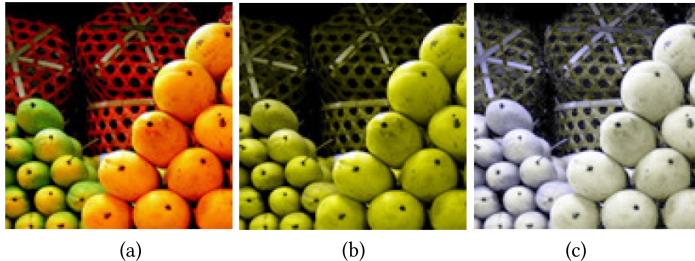


Fig. 4. LMS-based recoloring method in Reference [44]: (a) original image; (b) deutanope image view; (c) deutanope image view after recoloring. Reproduced from Reference [44] with permission from its authors.

quite rare. Note that, according to \mathbf{M} , each value of R' , G' , and B' is a linear combination of (R, G, B) , so (R', G', B') does not overflow the limits of the RGB color space.

Analysis of perceptual metrics: The compensation in the recoloring process is determined by the protanomaly degree α for protan trichromats and deutanomaly degree β for deutan trichromats. For example, a glance at matrix \mathbf{M} allows us to conclude that reds remain untouched for red-weak vision people (i.e., protans), because $\beta = 0$; the compensation of reds requires changing the values of G and B . Consequently, as shown in Figure 4, there is an increase in contrast that allows for distinguishing two distinct types of fruit, but the naturalness suffers, because all pixels are affected by the recoloring procedure. Nevertheless, color consistency is preserved, because \mathbf{M} maps each pixel color to another unique color.

Flatla-Gutwin method [20]. Similarly to Reference [45], the Flatla-Gutwin method is also customizable for each CVD person and requires a preliminary diagnosis, during which one identifies the set of distinctive colors as seen by such a person. Therefore, this method strikes on the colors that each person recognizes as distinct, i.e., his/her customized color domain.

The recoloring process takes into account such a customized color domain and is as follows. First, one extracts the set of key colors from a given image through quantization; for example, one uses a single key red for a set of similar reds in the image. Second, one determines the subset of confusing key colors by matching key colors with the colors of the customized color domain. Finally, one replaces each confusing key color by another color of the customized color domain to ensure color differentiability. Note that the pixels corresponding to non-confusing key colors are left untouched.

Analysis of perceptual metrics: The Flatla-Gutwin method focuses on color differentiability relative to confusing colors, so it enhances color contrast. However, it does not preserve color consistency across an image dataset, because a confusing key color does not always map to the same color. This color mapping depends on the other key colors in the image. Also, color naturalness holds, because the pixel colors associated with non-confusing key colors remain untouched.

3.3 HSx-based Methods

Although the RGB is the standard color format in display devices, it does not comply with the way the human brain tends to organize and interpret colors. On the contrary, HSx color models (HSI, HSL, and HSV) are known as *mind representations of colors* [82]; color components are the hue (H), saturation (S), and brightness (i.e., intensity (I), lightness (L), or value (V))). Regarding these HSx models, we can say that anomalous trichromat people perceive colors in a faded manner, i.e., the hues loose vivacity. This decolorization process translates into less saturated, darker colors

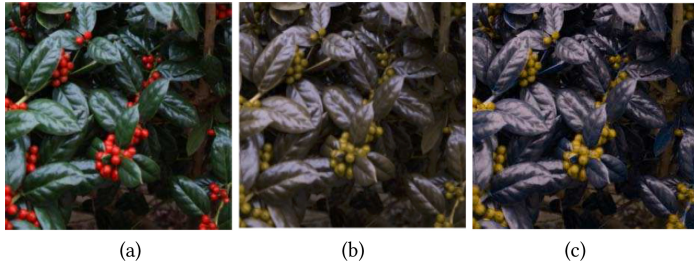


Fig. 5. HSV-based recoloring method in Reference [30]: (a) original image; (b) deutanope image view; (c) deutanope image view after recoloring. Reproduced from Reference [30] with permission from its authors.

(i.e., different chroma), yet the hue remains unchanged, which leads to a reduction of the image contrast. Therefore, the methods of this category operate in a way to recover the saturation and brightness as much as possible.

Chen-Liao method [11]. The pipeline of this recoloring method is $(R, G, B) \rightarrow (H, S, I) \xrightarrow{M} (H, S', I) \rightarrow (R', G', B')$, where M is the scaling matrix that only affects color saturation. That is, increasing the saturation from S to S' enhances color purity. After a careful experimental study, Chen and Liao concluded that an increase of 20% in saturation (i.e., $S' = 1.2 S$) is optimal; that is, the value $S' = 1.2 S$ ensures not only a better contrast but also a minimal change in color naturalness, even though all pixels are slightly affected by the recoloring process. Based on this optimal saturation value, Chen and Liao were able to simplify their recoloring pipeline to $(R, G, B) \rightarrow (R', G', B')$, so avoiding the explicit RGB-to-HSI and HSI-to-RGB conversions, and, consequently, speeding up the time performance.

Analysis of perceptual metrics: The color compensation method in Chen and Liao [11] takes advantage of the optimal saturation value $1.2S$ to enhance contrast for protans (anomalous red cones) and deutans (anomalous green cones), that is, for those with difficulties in discriminating between red and green hues. Color consistency is ensured by the matrix M . Furthermore, the optimal saturation value guarantees that color naturalness changes are kept at a minimum, though image artifacts may occur in little-saturated regions and with light reflections. This is so because the Chen-Liao method does not consider the image contents; that is, it blindly applies to all pixels.

Huang et al.'s method [30]. This method applies to both anomalous trichromacy and dichromacy. It is compensation recoloring method by remapping the hue components in the HSV color space. The saturation (S) and luminance (V) components remain unchanged to guarantee the naturalness of the re-colored image as much as possible, because they are not the main contributors to color confusion of CVD people. Therefore, the recoloring pipeline is as follows: $(R, G, B) \rightarrow (H, S, V) \rightarrow (H', S, V) \rightarrow (R', G', B')$. The remapping of the hue components in the HSV color space is performed using a histogram transformation [24], which has the effect of enhancing the hue contrast (Figure 5).

Analysis of perceptual metrics: Huang et al.'s method gets a better hue contrast as a result of the hue stretching. However, hue stretching translates itself into a counterclockwise rotation of hues in the HSV color space. Therefore, color naturalness may not be held for all images, because the hue rotation may result in an entirely different hue. Even worse is the fact that color consistency is not preserved at all, because the remapping of a given hue depends on the frequency (i.e., number of times) of each hue in the image.

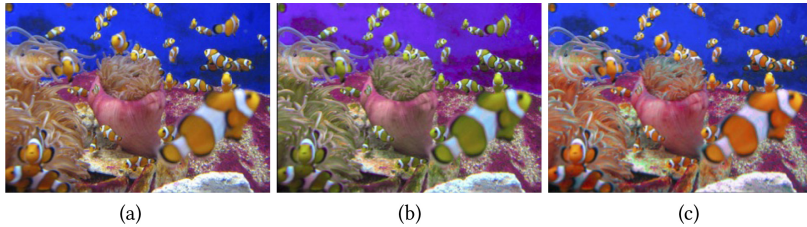


Fig. 6. CIE XYZ-based recoloring method in Reference [55]: (a) original image; (b) anomalous trichromat view; (c) anomalous trichromat view after recoloring. Reproduced from Reference [55] with permission from its authors (©2008 IS&T).

3.4 CIE-based Methods

Commission Internationale de l’Éclairage (CIE) color spaces preserve the perceptual uniformity, i.e., the distance between two colors corresponds to their perceptual difference [22]. Indeed, most works using these colors spaces build upon color distance to measure the augment of the discrimination among colors or to appraise how much a given color is different from the original.

3.4.1 CIE XYZ. Similarly to LMS, the CIE XYZ color space represents all colors seen by a human viewer. That is, the CIE XYZ color space is device independent. But, the CIE XYZ is richer than LMS, because it includes the luminance Y (i.e., “intensity of light,” not perceived luminance), in addition to the X and Z chromaticity parameters. Therefore, we can quantify the difference between, for example, a light red and a dark red [18]. However, XYZ is only perceptually uniform in the Riemann space, not in the Euclidean space. That is, small changes in XYZ may not result in small perceptual changes if one uses the Euclidean distance.

Mochizuki et al.’s method [55] (see also its follow-ups, References [62], [56], and [57]). This color compensation method relies on Riemann geometry. Its pipeline $(R, G, B) \xrightarrow{\text{M}^{-1}} (X, Y, Z) \xrightarrow{\text{M}^{-1}} (X', Y', Z') \rightarrow (R, G, B)$ provides anomalous trichromats (i.e., color-weak people) the same color perception as color-normal trichromats, where the matrix \mathbf{M} is the Riemann transformation metric that maps colors from the normal trichromat color space CIE XYZ to the (distorted) anomalous trichromat color space CIE X'Y'Z', which is basically a transformation from a sphere (a Riemann space) to an ellipsoid (another Riemann space), respectively. Indeed, a trichromat cannot distinguish each color from its neighboring colors within a threshold distance (i.e., within a spherical neighborhood) in the CIE XYZ color space and is called just-noticeable-difference (JND) threshold; for an anomalous trichromat, such an indistinguishable neighborhood of colors is an ellipsoid. Thus, to correct an image for an anomalous trichromat, we first calculate the inverse matrix \mathbf{M}^{-1} , called compensation matrix, applying then \mathbf{M}^{-1} to an image before presenting it to an anomalous trichromat viewer. The anomalous trichromat viewer perceives the preprocessed corrected image as the original image (see Figure 6(c)). Conversely, applying \mathbf{M} to the original image makes an ordinary trichromat viewer to see it as an anomalous trichromat observer (see Figure 6(b)).

Analysis of perceptual metrics: Mochizuki et al.’s method enables anomalous trichromats to see as normal trichromats. So, from the normal trichromat’s standpoint, color naturalness is recovered, though this may conflict with the perceptual experience of an anomalous trichromat person; for example, the background lilac in Figure 6(b) is seen as a blue in Figure 6(c) after image recoloring. However, colors do not change to distant colors because of the mapping from ellipsoids in the CIE X'Y'Z' color space to spheres in the CIE XYZ color space. As a consequence, the contrast is also recovered relative to normal trichromats. Furthermore, color consistency is ensured, because a given color is always mapped to the same color using \mathbf{M}^{-1} (cf. Figure 6).

3.4.2 CIE Luv. There are three main recoloring methods based on the CIE Luv color space, namely References [34], [63], and [53].

Ichikawa et al.’s method [34]. This compensation method is a follow-up of the one described in Reference [33]. Its pipeline is as follows: $(R, G, B) \xrightarrow{\text{RBC}} (L, u, v) \xrightarrow{\text{RBC}} (L', u', v') \xrightarrow{\text{RBC}} (R', G', B')$. Ichikawa et al.’s method aims to improve the discrimination among confusing colors, while keeping the image naturalness as much as possible. Ichikawa et al.’s method builds upon a kind of color segmentation with connectivity information (i.e., parenthood and brotherhood relations between image regions). First, one uses the median-cut algorithm to quantize all colors in a given image into n key colors (c_1, c_2, \dots, c_n). Then, each pixel color is categorized as belonging to the image region R_k ($k = 1, \dots, n$) if its distance to c_k is the smallest one among all key colors. After color segmentation of the image, one uses a genetic algorithm—specifically, the random bit climbing (RBC) algorithm—that iteratively produces an optimal color vector $(c'_1, c'_2, \dots, c'_n)$ from the original vector (c_1, c_2, \dots, c_n) .

Such genetic algorithm sustains on a fitness function that attains a minimum after some iterations. However, only the key colors are subject to correction to distinguish key colors that are indistinguishable for anomalous trichromat people. Finally, based on the optimal key colors $(c'_1, c'_2, \dots, c'_n)$, all image pixels are recolored accordingly.

Analysis of perceptual metrics: Ichikawa et al.’s method [34] is contrast oriented, but it does not preserve color consistency, because the final (optimal) key colors depend on the initial key colors and their mutual relations in a given image. Although the optimization procedure requires a prior quantification of color discrimination degree (i.e., severity degree) of each anomalous trichromat person, the naturalness cannot be ensured, because color quantization may lead to image artifacts, unless the number of key colors is sufficient, particularly in images with chromatic diversity. That is, insufficient quantization undermines the image naturalness.

Oshima et al.’s method [38, 63, 64]. This color compensation method is a follow-up of the work in Mochizuki et al. [55] described above, but it uses the CIE Luv instead of the CIE XYZ color space. Therefore, its recoloring pipeline is as follows: $(R, G, B) \xrightarrow{\text{M}^{-1}} (L, u, v) \xrightarrow{\text{M}^{-1}} (L', u', v') \xrightarrow{\text{M}^{-1}} (R', G', B')$, where M^{-1} is the compensation matrix, and (L', u', v') is the adapted color that enables an anomalous trichromat person to see (L, u, v) as for a color-normal trichromat person. Note that Oshima et al. were able to determine the color distortion matrix M that maps colors from the CIE Luv color space (as seen by color-normal trichromats) to the distorted CIE Luv color space (as seen by anomalous trichromats). In fact, and similarly to Reference [55], M transforms a sphere into an ellipsoid. To enable an anomalous trichromat to see as a normal trichromat, one applies the inverse transformation M^{-1} to the original image. Such mapping transforms an ellipsoid into a sphere centered at each color in the CIE Luv color space.

Analysis of perceptual metrics: Oshima et al.’s method has the advantage of using the CIE Luv color space, which is perceptually uniform so that the computation of the matrix M is more rigorous than the one in Mochizuki et al. [55]. Consequently, color contrast gets enhanced, and color consistency holds. Similarly to Mochizuki et al.’s method, the recoloring method in Oshima et al. enables anomalous trichromats to see a recolored image like color-normal trichromats see the original image. Thus, color naturalness is preserved from the color-normal trichromat’s standpoint, but not necessarily from anomalous trichromat’s point of view.

Milic et al.’s method [53]. This image content-dependent method has the following pipeline: $(R, G, B) \xrightarrow{\text{NBR}} (L, u, v) \xrightarrow{\text{NBR}} (L', u', v') \xrightarrow{\text{NBR}} (R', G', B')$. It is a neighborhood-based recoloring (NBR) method, because confusing colors are mapped to neighboring colors in the CIE Luv color space.

Given a subset of confusion colors, Milic et al. adopted the strategy of keeping only one of them in the confusion line; the remaining ones are shifted perpendicularly to the confusion line. This NBR method consists of three steps. First, one carries out a color image segmentation based on (u, v) -chromaticity, using k -means clustering to form clusters of colors, whose centers are the key colors of the input image. Note that this step excludes the lightness (L) from the color segmentation-and-clustering process. Second, the recoloring process of the key colors takes place. When two or more of these colors lie on the same confusion line, all except one should be rotated around the confusion point (i.e., the convergence point of all the confusion lines in CIE Luv color space) to a neighboring color to create room for color differences. Third, recoloring each pixel takes place preserving relative to its adapted representative color, though preserving their original color difference.

Analysis of perceptual metrics: Milic et al.'s method ensures color contrast, because its focus is on creating color differences perpendicularly to confusion lines in the CIE Luv color space. Color naturalness also holds, because the rotation of each confusing color occurs inside one of its small neighborhoods in the CIE Luv color space. Note that color remapping only takes place for confusing colors; the remaining ones are left untouched. Color consistency does not hold, because the recoloring process depends on the colors and color segments present in the original image, but its effect becomes irrelevant, because the recoloring process always occurs inside a small neighborhood of each original color.

3.4.3 CIECAM. Seemingly, the only recoloring method that relies on the CIECAM color space was recently proposed by Nuñez et al. [61]. CAM is the shorthand for color appearance model introduced in 1997 by the CIE Technical Committee 8-01 (Color Appearance Modelling for Color Management Systems) with the purpose of accurately modeling the human color perception [47]. The CIECAM97 was later reformulated to give rise to CIECAM02-UCS Jab color space [46], which is perceptually uniform; note that UCS stands for uniform color space. Perceptual uniformity means that colors change at a constant rate, preventing colors in color space from changing too slowly or too quickly relative to human color perception. In other words, the Euclidean distance between colors in CIECAM02-UCS Jab is congruent with the human perception of color difference. This color space defines color in terms of lightness (J), red-to-green correlate (a), and blue-to-yellow correlate (b).

Nuñez et al.'s method. This is described in Reference [61] and relies on CIECAM02-UCS Jab color space. Its pipeline $(R, G, B) \rightarrow (J, a, b) \xrightarrow{\Delta J, \Delta a, \Delta b} (J', a', b') \rightarrow (R', G', B')$, where $(\Delta J, \Delta a, \Delta b)$ represent the color compensation to ensure that an anomalous trichromat and a color-normal trichromat perceive the same color, at least approximately, when they observe (R', G', B') and (R, G, B) , respectively. The computation of $(\Delta J, \Delta a, \Delta b)$ requires to convert the RGB color as seen by a color-normal trichromat into RGB color as viewed by an anomalous trichromat, which is performed using the CVD simulation model introduced in Reference [51]. Smith [80] describes how to achieve the color conversion between RGB and CIECAM02-UCS Jab.

However, after the color compensation in CIECAM02-UCS Jab color space, the color mapping back to RGB color space may produce out-of-range RGB components, particularly when the user is dealing with colormaps in scientific visualization. This problem is similar to the one discussed in Reference [94] in the context of LMS-to-RGB conversion (see Section 3.1). To overcome this problem, one proceeds to the following operations before getting back to RGB color space: (i) linearization and maximization of the J range of the colormap and (ii) interpolation of the a range (and b range) of the colormap to generate equidistant points or colors. Additionally, to avoid computing invalid or out-of-range RGB colors, Nuñez et al. used a gamut mapping based on an absolute

colorimetric rendering intent [59, 79] to guarantee that all RGB component values lie in the range $[0, 1]$ rather than $[0, 255]$.

Analysis of perceptual metrics: As in Mochizuki et al. [55], Nuñez et al.'s method makes both color-normal and anomalous trichromats see every single color as the same color or nearly the same color. Thus, from the color-normal trichromat standpoint, color naturalness holds, but not necessarily from the anomalous trichromat point of view. The color compensation strategy also has the effect of restoring color contrast given the perceptual uniformity of CIECAM02-UCS. Color consistency is also maintained, because mappings (via matrix transformations) between RGB and CIECAM02-UCS color spaces, and back, ensure that the resulting colors are unique and valid.

3.5 YCC-based Methods

These methods rely on the family of YCC color spaces, namely YCbCr and Y'CbCr, which usually incorporate the color image pipeline of digital photography systems, as well as video systems. In YCbCr, the Y stands for the brightness (luminance or luma), Cb the blue minus luma ($B - Y$), and Cr the red minus luma ($R - Y$); recall that $Y = 0.2126 R + 0.7152 G + 0.0722 B$; Y'CbCr differs from YCbCr in that Y' is the value of luminance with gamma correction. Note that, while Y represents physical linear-space brightness, Y' represents the (nonlinear) perceptual brightness. We found only one recoloring method based on YCbCr in the literature, as described in the sequel.

Woo et al.'s method [91]. This color compensation method applies to anomalous trichromats, in particular, protan and deutan trichromats. It takes place in the YCbCr color space and has the following pipeline: $(R, G, B) \rightarrow (Y, Cb, Cr) \xrightarrow{\Delta h, \Delta C} (Y, Cb', Cr') \rightarrow (R', G', B')$. Note that the luminance Y remains unchanged, because the luminance difference perceived by trichromats and anomalous trichromats is small. For the sake of minimizing the complexity, the computation of color compensation takes place in the CIE LCh (luminance, chrominance, and hue angle) color space, with $C = \sqrt{Cb^2 + Cr^2}$ and $h = \arctan(Cr/Cb)$, which is perceptually uniform. Similarly, one needs to calculate the homologous chroma $c = \sqrt{cb^2 + cr^2}$ and hue angle $a = \arctan(cr/cb)$ as seen by an anomalous trichromat, which requires the prior computation of homologous (r, g, b) as seen by an anomalous trichromat. Color compensation then consists of adding the hue angle difference $\Delta h = h - a$ to h and chroma difference $\Delta C = C - c$ to C ; the resulting h' and C' allow for finding Cb' and Cr' . Thus, an anomalous trichromat sees (Y, Cb', Cr') as an ordinary trichromat sees (Y, Cb, Cr) ; that is, both individuals see the same color, much like in Mochizuki et al. [55].

Analysis of perceptual metrics: Similarly to Reference [55], Woo et al.'s method makes anomalous trichromats see colors in the same manner as color-normal trichromats; that is, it preserves the color naturalness from the color-normal trichromat's point of view but not necessarily from the anomalous trichromat's point of view. Note that color compensation takes advantage of the perceptual uniformity of the CIE LCh, so one restores color contrast. Also, color consistency is maintained because of the (matrix) transformations between color spaces.

3.6 Methods for Anomalous Trichromacy: A Discussion

A brief glance at Table 1 shows the following:

- *Anomalous trichromacy types.* Most recoloring methods apply to the three types of anomalous trichromacy. Indeed, anomalous trichromats see all colors, yet in a distorted way, as a consequence of malfunctioning of one kind of cones. So we need to compensate or correct the color distortion caused by such cones, independently of the type of anomalous trichromacy.

Table 1. Recoloring Methods for Anomalous Trichromat People

Reference	Anomalous trichromacy			Other CVDs	Color space	Target media			Color range	Method type	Perceptual metrics				
	P	D	T			I	D	H			M	O	CE	CC	NP
Yang and Ro [92]	•	•	•		LMS	•			TC	•			•	•	•
Ichikawa et al. [33]	•	•			Luv		•		key		•		•	•	•
Ichikawa et al. [34]	•	•			Luv	•			key		•		•	•	•
Yang et al. [93]	•	•	•		LMS	•			TC	•			•	•	•
Yang et al. [94]	•	•	•		LMS	•			TC	•			•	•	•
Mochizuki et al. [55]	•	•	•		XYZ	•			TC	•			•	•	•
Poret et al. [67]	•				RGB	•			TC	•			•	•	•
Oshima et al. [62]	•	•	•		XYZ	•			TC	•			•	•	•
Lee and Santos [44]	•	•		•	RGB	•			TC	•			•	•	•
Lee and Santos [45]	•	•		•	RGB	•			TC	•			•	•	•
Mochizuki et al. [56]	•	•	•		XYZ	•			TC	•			•	•	•
Mochizuki et al. [57]	•	•	•		XYZ	•			TC	•			•	•	•
Chen and Liao [11]	•	•			HSI	•			TC	•			•	•	•
Flatla and Gutwin [20]	•	•	•	•	RGB	•	•		key		•		•	•	•
Oshima et al. [63]	•	•	•		Luv	•			TC	•			•	•	•
Kojima et al. [38]	•	•	•		Luv	•			TC	•			•	•	•
Milic et al. [53]	•	•	•	•	Luv	•			key	•			•	•	•
Oshima et al. [64]	•	•	•		Luv	•			TC	•			•	•	•
Nuñez et al. [61]	•	•	•		CIECAM	•			TC	•			•	•	•
Woo et al. [91]	•	•			YCbCr	•			TC	•			•	•	•

Abbreviations:

Anomalous trichromacy: P (protanomaly); D (deuteranomaly); T (tritanomaly).

Other CVDs: dichromacy or monochromacy.

Target media: I (still images or video); D (drawings and charts); H (HTML documents).

Color range: TC (true color); key (key color).

Method type: M (matrix-based); O (optimization-based).

Perceptual metrics: CE (contrast enhancement); CC (color consistency); NP (naturalness preservation).

- *Other CVDs.* Some of the recoloring methods for anomalous trichromacy also apply to dichromacy or monochromacy.
- *Color spaces.* Most recoloring methods build upon on CIE color spaces (11 of 20). To some extent, this is because the color spaces CIE color spaces enjoy the color uniformity property. Specifically, the distance between colors in the CIE Lab and CIE Luv color spaces is the Euclidean distance. Thus, the Euclidean distance can be used as a metric to measure and ensure color contrast between confusing colors in images as seen by anomalous trichromats. Interestingly, no method takes advantage of the CIE Lab color space. However, the CIE XYZ space has the advantage of being device independent, but it is not perceptually uniform when one uses the Euclidean distance. However, it is perceptually uniform when one uses the Riemann metrics (see, for example, Reference [55]).
- *Target media.* All methods, except the one in Ichikawa et al. [33], were designed for still images. However, there is a widespread understanding that any recoloring method must not depend on the medium, either it is an image, an HTML document, text, or even video; hence, the focus on still images.
- *Color ranges and method types.* The color range used by a given method is closely related to the color compensation technique. Mainly, we have identified two main color compensation

techniques: *objective function optimization* and *matrix-based color remapping*. Typically, optimization-based methods use a small set of *key* (or representative) colors of the input image. Then, one uses color interpolation to remap the remaining colors. Most methods based on CIE color spaces use objective functions to iteratively maximize distances between confusing colors (i.e., enhancing the contrast), but at the same time to minimize such color changes to preserve the color naturalness as much as possible. Matrix-based methods use true colors (TC) to remap colors. Usually, these latter methods build upon any color space, but LMS, HSx, and RGB color spaces are predominant. They use a color remapping matrix, no matter if it is an inverse matrix or a rotation matrix or something else.

- *Perceptual metrics.* All methods focus on recovering the color contrast caused by the color distortion of the anomalous trichromacy condition. Most of these methods are color consistent and preserve color naturalness. That is, most methods hold the perceptual learning of anomalous trichromat people, because normal trichromats and low-severity anomalous trichromats own the same color gamut, yet the latter ones see color in a distorted manner. But, for high-severity anomalous trichromats, it is rather difficult or even impossible to recover the original colors seen by a color-normal trichromat. Indeed, their color gamut drastically reduces itself when the severity degree increases to its maximum at 1, which amounts to the dichromacy condition.

Thus, the main conclusions we can draw from the state-of-the-art methods for anomalous trichromats are the following:

- Both matrix-based and optimization-based recoloring methods allow for the correction of color distortion of low-severity anomalous trichromats, because low-severity anomalous trichromats and color-normal trichromats have the same color gamut. In other words, it is feasible to make them see as color-normal trichromats.
- Except for the methods in Lee and Santos [44, 45] and Flatla and Gutwin [20], most methods do not consider the severity degree of the color anomaly of each anomalous trichromat person. Consequently, often the color correction is not performed suitably.
- Apart from the methods in Flatla and Gutwin [20] and Milic et al. [53], most methods operate in a pixelwise manner; that is, they are content independent. On the contrary, those two methods first identify confusing colors, and only these are subject to the recoloring procedure; that is, they are content dependent.

In general, matrix-based and optimization-based recoloring methods preserve the perceptual learning of anomalous trichromat people, because one assumes that the color distortion is tractable and can be corrected. The ultimate objective is thus to make anomalous trichromats to see as color-normal trichromats.

4 CVD RECOLORING METHODS FOR DICHROMACY

In spite of anomalous trichromat people seeing in a distorted way, as a consequence of the peak sensitivity shift of their defective cones, their color space is 3D. However, dichromat people's color space reduces to a 2D plane, because their cones of a specific type do not work at all or are absent in the retina. Consequently, 3D colors project themselves onto a 2D plane, causing color overlapping and confusion to dichromat people. The idea is then to diminish such confusion by remapping and setting apart the most confusing colors (i.e., reds and greens). Note that, unlike recoloring methods for anomalous trichromats, there is no room for color compensation for dichromats.

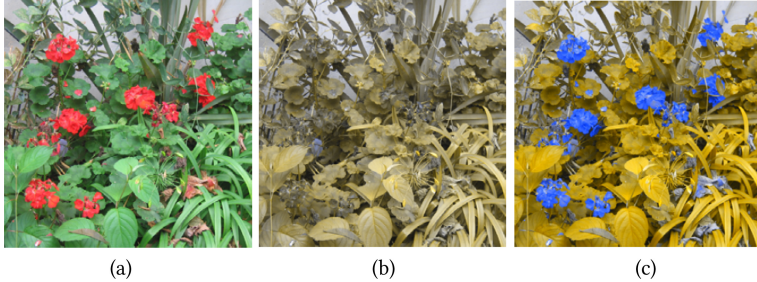


Fig. 7. LMS-based recoloring method in Reference [36]: (a) original image; (b) deutan image view; (c) deutan image view after recoloring. Reproduced from Reference [36] with permission from the authors (©2007 ACM).

4.1 LMS-based Methods

Dichromacy means that one of the parameters L , M , or S takes on the value zero; for example, a deuteranope person sees the color (L, M, S) as $(L, 0, S)$. That is, a deuteranope person perceives no variation on the M axis so that color stimuli with fixed L , varying M , and fixed S collapse to the same color $(L, 0, S)$. We found two main LMS-based recoloring methods for dichromacy, which are in Jefferson and Harvey [36] and Chen et al. [10]. Nevertheless, another method introduced by Ma et al. [48] proposes a back-propagation neural network (BPNN) model to simulate the colorblindness cure. This proposal suffers from practicability issues that are difficult to overcome given the current state-of-the-art of vision science and technology unless one finds a way to stimulate the non-responsive cones in the retina or their corresponding neurons in the brain.

Jefferson-Harvey method. As described in Reference [36], the pipeline of this method is as follows: $(R, G, B) \xrightarrow{\text{recoloring}} (L, M, S) \rightarrow (L', M', S') \rightarrow (R', G', B')$. Its recoloring mapping regulates itself by the following transformation:

$$\begin{bmatrix} L' \\ M' \\ S' \end{bmatrix} = \underbrace{\begin{bmatrix} L \\ M \\ S \end{bmatrix} + \begin{bmatrix} 1 & a_{12} & a_{13} \\ a_{21} & 1 & a_{23} \\ a_{31} & a_{32} & 1 \end{bmatrix} \cdot \left(\begin{bmatrix} L \\ M \\ S \end{bmatrix} - \begin{bmatrix} l \\ m \\ s \end{bmatrix} \right)}_{\Delta C}, \quad (1)$$

where ΔC stands for the difference between the original color (L, M, S) and simulated dichromat color (l, m, s) obtained through Brettel et al.'s algorithm [7, 86]. As Equation (1) shows, the fundamental idea of the Jefferson-Harvey algorithm is to transfer the chromatic data of the missing cone type over the two functioning cone types. Thus, this algorithm focuses on the color distinguishability as of ΔC . The matrix A depends on the CVD type; $a_{12} = a_{13} = 0$ for protanopia, $a_{21} = a_{23} = 0$ for deutanopia, and $a_{31} = a_{32} = 0$ for tritanopia. The non-null components of A are found in an interactive manner for each dichromat person using a correction slider of a GUI interface. Therefore, the method is not automated.

Analysis of perceptual metrics: With the Jefferson-Harvey method, the contrast increases at the cost of less naturalness. To guarantee color distinguishability, some colors are mapped to other entirely different colors, as shown in Figure 7. Such color distinguishability results from the difference ΔC between the original color (L, M, S) and the homologous color (l, m, s) perceived by a dichromat person. Nevertheless, the color consistency holds, since the matrix A remains unchanged for each user.

Chen et al.'s method. As described in Reference [10], this method proposed a direct volume rendering (DVR) approach for dichromats in the context of medical imageology. The underlying

pipeline is as follows: $(R, G, B) \xrightarrow{\text{recoloring}} (L, M, S) \xrightarrow{\text{recoloring}} (L', M', S') \xrightarrow{\text{recoloring}} (R', G', B')$. As for the previous method, the recoloring procedure requires the conversion from each (L, M, S) color to (l, m, s) color, as perceived by normal trichromat and dichromat people, respectively. Taking into consideration that dichromat people only possess two functional types of cones, their color space reduces to two half-planes, where the first concerns blueish colors while the second concerns yellowish ones. So, the algorithm was developed to distinguish blues from blues and yellows from yellows, mainly when two adjacent anatomical organs are color indistinguishable. Color distinguishability is performed using distinct opacity values as coefficients in the linear combination of two colors (two organs) considering the geodesic distance between them on the two half-planes. Recoloring thus reduces to a linear combination that transforms (l, m, s) into (L', M', S') in the dichromat color space.

Analysis of perceptual metrics: In medical imaging based on the dichromat color space, it is essential to preserve details (i.e., contrast), as well as semi-transparent effects for overlapping organs to better distinguish them in a perceptually natural manner. Indeed, color-indistinguishable anatomical organs end up getting distinct using different color opacities. These distinct opacities also ensure a noticeable color contrast. Furthermore, the recoloring procedure underpinning the Chen et al.'s method produces a unique color from the linear combination of any two colors concerning the geodesic distance on the dichromat's LMS color space (i., two half-planes), so color consistency holds.

4.2 RGB-based Methods

There are six RGB-based recoloring methods in the literature: References [35] and [1] (and its follow-ups [17, 37]) and References [16], [2], [49], and [74]). Recall that the Flatla-Gutwin method [20] described in Section 3.2 also applies to dichromacy.

Jefferson-Harvey method [35]. This recoloring method builds upon the minimization of the objective (or error) function defined in the RGB color space. It consists of four steps: (i) color sampling of the input RGB image to obtain its key colors; (ii) computing target distances between key colors; (iii) minimization of the objective function; and (iv) interpolation between the corrected key colors to find the remaining colors in the recolored image. In the first step, one extracts the set of key colors of a given image by color sampling based on the difference histogram. The small number of key colors helps to speed up the optimization procedure in the third step; otherwise, it might be quite slow. In the second step, one computes the target distances between key colors that must be preserved in optimization step to guarantee that a CVD person does not lose any image details seen by a normal-vision trichromat. In conformity with W3C/WAI accessibility evaluation criteria, the target distance between two colors c_i and c_j is given by $D(c_i, c_j) = \alpha_1 \cdot \|c_i - c_j\|_1 + \alpha_2 \cdot |Y(c_i) - Y(c_j)|$, where $\|c_i - c_j\|_1$ denotes the Manhattan distance between c_i and c_j , $|Y(c_i) - Y(c_j)|$ the absolute value of their luminance difference in the YIQ color space, and α_1 and α_2 the color and luminance difference weights. In the third step, the remapping of the key colors takes place in terms of the minimization of the error (or objective) function $f = \varepsilon_1 + \varepsilon_2 + \varepsilon_3$, where ε_1 , ε_2 , and ε_3 are subsidiary error functions. The idea of this optimization step is to preserve the contrast and brightness (luminance), so the first error function $\varepsilon_1 = \frac{1}{\sum_{i < j} D(i, j)} \sum_{i < j}^n (D(c_i, c_j) - D(d_i, d_j))^2$, where n is the number of key colors and (d_i, d_j) are the homologous colors of (c_i, c_j) remapped onto the color space of CVD people. Note that ε_1 can be seen as a Sammon error measure as used in multidimensional scaling [14]. In turn, the method minimizes the gamut error ε_2 and the error component ε_3 that penalizes the incorrect mapping of particular colors like black and white that must remain unchanged.

Analysis of perceptual metrics: The idea underlying the Jefferson-Harvey method [35] is to preserve the contrast and brightness by keeping the distance between any pair of remapped key colors as much as possible identical to the distance between their original key colors, as represented by the first error function ϵ_1 . But color consistency does not hold, because the key colors vary from an image to another; consequently, color naturalness does not maintain either.

Anagnostopoulos et al.’s method. As noted in Reference [1], this method applies to protanope people. Its leading idea is similar to that introduced by Jefferson and Harvey [36] (see Section 4.1). However, the recoloring procedure takes place in the RGB color space rather than in LMS color space. Such an iterative recoloring procedure is performed by iteratively modifying the 3×3 discrimination matrix M , so the remapped color is given by:

$$\begin{bmatrix} R' \\ G' \\ B' \end{bmatrix} = \underbrace{\begin{bmatrix} R \\ G \\ B \end{bmatrix}}_M + \underbrace{\begin{bmatrix} -1 & 0 & 0 \\ \alpha & 1 & 0 \\ \beta & 0 & 1 \end{bmatrix}}_{\Delta C} \cdot \left(\begin{bmatrix} R \\ G \\ B \end{bmatrix} - \begin{bmatrix} r \\ g \\ b \end{bmatrix} \right), \quad (2)$$

where ΔC is the color error between the original color (R, G, B) and the homologous protanope color (r, g, b) associated to a given pixel; the color (r, g, b) is obtained through the simulation algorithm for protanopes, as described by Brettel et al. [7]. Anagnostopoulos et al. assert that the color (r, g, b) seen by a protanope person is correct if the error $\Delta C = (R - r, G - g, B - b) \leq 0.01 (R, G, B)$; otherwise, incorrect pixels colors are subject to an iterative recoloring procedure such that the discrimination matrix M is initialized with $\alpha = \beta = 1$; the value of α (respectively, β) decreases (respectively, increases) by 0.05 in each iteration under the condition $\sum_{i=1}^9 m_i = 3$, where m_i denotes the i th component of M . This iterative procedure stops when all remapped colors are distinguishable from each other. This recoloring procedure leads to a gradual reduction of R in favor of G and B . As a result, we obtain less saturated reds/oranges (i.e., dark grays as seen by protanope people become less dark grays), while greens get more saturated, mitigating their red-green confusion.

Analysis of perceptual metrics: Anagnostopoulos et al.’s method improves color contrast in images, because the color disambiguation is performed iteratively by changing α and β in M . However, the color consistency does not maintain, because the adjustment of a given color depends on the color gamut of the image. In general, colors do not change their chromaticity in a significant manner, though the loss of chromaticity is more noticeable in the reds (i.e., the confusing colors), so that color naturalness changes are only slightly significant. In Doliotis et al. [17] (a follow-up of Anagnostopoulos et al.’s method), the naturalness is reinforced as only colors perceived differently by protanopes are subject to recoloring.

Deng et al.’s method [16]. This recoloring method first maps the 3D RGB color space (i.e., a cube) onto the dichromat’s 2D RGB color space. This mapping is not linear, so each point in 2D dichromat color space does not correspond to a confusion line (i.e., a color line that collapse to a single color). On the contrary, the dimension-reduction mapping builds upon Sammon’s non-linear mapping [77], though preserving the structure of 3D inter-point distances in the 2D plane projection.

The pipeline $(R, G, B) \xrightarrow{\text{discretization}} (r, g, b) \xrightarrow{\text{mapping}} (r', g', b')$ of Deng et al.’s method has two main steps. First, one divides uniformly (i.e., a grid of equally-spaced nodes) both the 3D trichromat and 2D dichromat color spaces with the same number of nodes. In a way, each grid node can be seen as a key color (r, g, b) or a small cube featuring the just-noticeable-difference (JND) threshold that measures the minimal color-difference that the observer can detect. Such 3D and 2D grids of colors were named similarity matrices, because they are used to assess the similarity of

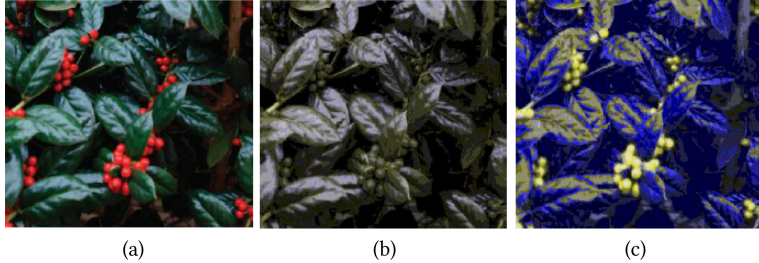


Fig. 8. RGB-based recoloring method in Reference [16]: (a) original image; (b) deutanope image view; (c) deutanope image view after recoloring. Reproduced from Reference [16] with permission from Springer (©2007 Springer).

color-to-color distance relations between such discrete 3D and 2D space structures. Second, one uses a distance minimization procedure (e.g., steepest descent procedure) between homologous points in both spaces to maintain as much as possible the ratio of distances between those homologous points. This (r, g, b) -to- (r', g', b') mapping between homologous colors gets encoded into a unique look-up table, which applies to any image.

Analysis of perceptual metrics: The look-up table ensures the consistency of the recoloring procedure. However, preserving distance ratios guarantees the necessary color contrast, yet at the cost of loss of naturalness, as illustrated in Figure 8.

Ma et al.’s method. As described in Reference [49], this method is similar to the one in Deng et al. [16] but uses a different device. Specifically, it uses the self-organizing map (SOM) as its nonlinear color mapping, and it is also known as self-organizing feature map (SOFM). However, instead of uniformly sampling the RGB color space, Ma et al. make a random sampling of the input image itself, in the attempt of eliminating repetitive colors and, consequently, to speed up the recoloring procedure. Such nonlinear color mapping is an artificial neural network (ANN) model, which is here used to map a feature (e.g., an RGB color) from the 3D RGB color space onto the 2D dichromat plane. The ANN learns through unsupervised learning. Note that SOM enjoys two essential properties: First, the nonlinearity allows for better compression of the color space than linear ones; second, it preserves the neighboring relationships (and, inherently, the distance ratios) between colors. Therefore, the leading idea is to perform color mapping by preserving distance ratios between homologous colors of 3D and 2D color spaces, as a way of improving color discrimination in still images.

Analysis of perceptual metrics: Similarly to Deng et al. [16], there is a noticeable enhancement of color contrast, because distance ratios hold but at the cost of a loss of color naturalness. But, unlike Deng et al.’s method, color consistency does not hold because of the random sampling of the original image; that is, the color samples depend on the color gamut of the input image.

Bao et al.’s method [2]. This method aims to improve color discrimination of red-green dichromat people (protanopia and deutanopia), though preserving color naturalness. In its pipeline $(R, G, B) \rightarrow (R, G, B')$, the components R and G remain unchanged, but the blues change from B to B' , which depends on the location of the color (R, G, B) in relation to the dichromat plane defined by $R = G$:

$$B' = \begin{cases} B \frac{f_1}{f_1 + f_2} & \text{if } R > G \\ 255 \frac{f_1}{f_1 + f_2} + B \frac{f_2}{f_1 + f_2} & \text{if } R \leq G \end{cases}, \quad (3)$$

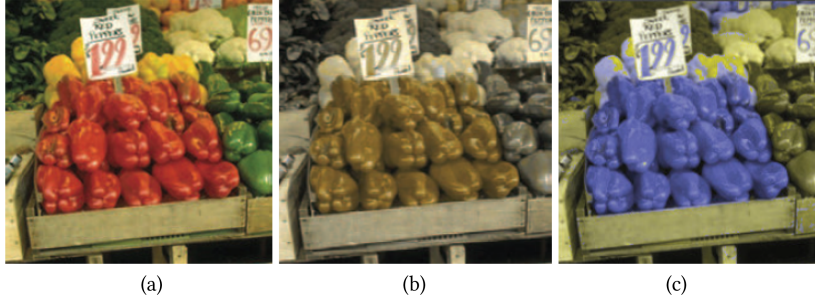


Fig. 9. RGB-based recoloring method in Reference [74]: (a) original image; (b) deutanope image view; (c) deutanope image view after recoloring. Reproduced from Reference [74] with permission from the IEEE (©2010 IEEE).

where f_1 is the number of pixels with $R > G$, while f_2 is the number of the remaining pixels in the image. According to Equation (3), a decrease in blue when $R > G$ and $R < B$ (i.e., violet purples) leads to a reduction of saturation and brightness, but, when $R > G$ and $R \geq B$ (i.e., magentas, reds, and oranges), it leads to an increase of saturation and a decrease of brightness. Also, in conformity with Equation (3), an increase in blue when $R \leq G$ and $R < B$ (i.e., cyans and blues) leads to an increase in saturation and brightness. But, when $R \leq G$ and $R \geq B$ (i.e., greens), it leads to a decrease of saturation and an increase in brightness. Thus, color discrimination improves by stressing the differences of saturation and brightness between colors behind and beyond the dichromat plane $R = G$. As a margin note, let us mention that Bao et al. proposed a similar recoloring procedure for yellow-blue dichromat people (tritanopy).

Analysis of perceptual metrics: Bao et al.'s method also focuses on contrast enhancement, but it is not consistent, since increasing/decreasing of B depends on the frequencies f_1 and f_2 in the input image. There is no naturalness preservation, because the recoloring procedure also applies to non-confusing colors.

Ruminski et al.'s method [74]. This recoloring method has the pipeline $(R, G, B) \rightarrow (r, g, b) \rightarrow (r', g', b') \rightarrow (R', G', B')$, where (r, g, b) stands for the normalized color of (R, G, B) . The recoloring procedure only takes place if the following conditions are satisfied: (i) $\Delta_{CIE} > 0.092$, where Δ_{CIE} denotes the CIE distance between each pixel color (R, G, B) of the original image and its homologous color as seen by a dichromat person; (ii) the hue of the color is not blue, yellow, or gray. Therefore, the recoloring essentially restricts to reds and greens, and is as follows:

$$\begin{bmatrix} r' \\ g' \\ b' \end{bmatrix} = \begin{bmatrix} r \\ g \\ 0 \end{bmatrix} + \begin{bmatrix} 0.5\Delta_{CIE} \\ -0.5\Delta_{CIE} \\ r^\gamma \end{bmatrix}, \quad (4)$$

where $\gamma = g$ represents the gamma correction; note that r , g , and b stand for normalized values of R , G , and B , respectively. According to Equation (4), reds become more saturated, while greens become less saturated; also, gamma correction makes the reds become closer to magentas and magentas closer to blues. As a consequence, the gamma correction associated with the blue channel aims to distinguish between original magentas and magentas introduced by red-to-blue mapping (see Figure 9).

Analysis of perceptual metrics: Ruminski et al.'s method does not preserve color naturalness, since the original reds are all seen as saturated blues, which provokes confusion with the original

blues. Thus, the contrast is not guaranteed when the image features plenty of reds and blues. Even so, Equation (4) ensures color consistency, since each color always maps to the same color.

4.3 HSx-based Methods

These methods build upon HSx color spaces, where H stands for hues, S saturation, and x brightness. Specifically, there are three HSx color spaces, namely HSI (I is the intensity), HSL (L stands for the lightness), and HSV (V represents the value). For dichromat people, each one of these 3D color spaces collapses to a 2D color space. In the case of deuteranomaly and protanomaly, the dichromat condition leads to a significant reduction of the image contrast, because all colors collapse onto the 60° (yellow) or 240° (blue) half-planes (see Figure 3(b) and (c)). In the case of tritanomaly, the projection is onto the 0° (red) or 180° (green) half-planes (see Figure 3(d)). Consequently, protanopes and deuteranopes only see yellows and blues, while tritanopes only see reds and cyans. That is, protanopes and deuteranopes mainly confuse reddish and greenish colors, while tritanopes get confused with yellowish and blueish colors. Thus, most HSx-based methods focus on discriminating these confusing hues.

4.3.1 HSI. In the literature, we found only one recoloring method based on HSI color space, as described in Reference [92].

Yang-Ro method [92]. This recoloring method is one of the first we may find in the literature (see Table 2). Its pipeline is as follows: $(R, G, B) \rightarrow (H, S, I) \xrightarrow{\text{recoloring}} (H', S', I') \rightarrow (R', G', B')$ such that

$$\begin{bmatrix} H' \\ S' \\ I' \end{bmatrix} = \begin{bmatrix} H \\ S \\ I \end{bmatrix} + \begin{bmatrix} \Delta h \\ \Delta s \\ 0 \end{bmatrix}, \quad (5)$$

where Δh and Δs are the hue and saturation variations used in the recoloring procedure; the intensity I remains unchanged. The leading idea is to remap H to another hue H' , applying then a saturation shift to distinguish between the new color (H', S', I) and other colors with the same hue H' in the input image.

In particular, considering protanomaly and deuteranomaly, the method rids off the confusion between greens and reds by remapping reddish colors (i.e., colors with $R > G, B$) to blueish colors (i.e., colors with $B > R, G$). However, this causes confusion between reddish and blueish colors. To mitigate this confusion, one decreases the saturation of the remapped hue. The hues of blueish colors are left untouched, but the remaining colors are subject to the following hue shift $\Delta h = h_{\max} \cdot \rho_M$, where h_{\max} is the pre-defined maximum hue shift, and ρ_M is the magenta ratio. This ratio represents the amount of magenta in a given color and attains its maximum at pure magenta ($G = 0$) and its minimum at pure green ($G = 255$), since magenta is the complement of green. In other words, the hue shift progressively increases from greens ($\Delta h = 0$) to magentas ($\Delta h = h_{\max}$), no matter if it is clockwise or counterclockwise.

In turn, the saturation shift $\Delta s = s_{M_{\max}} \cdot \rho_M + s_{C_{\max}} \cdot \rho_C$ applies to all pixel colors, where ρ_M and ρ_C represent the magenta and cyan ratios, while $s_{M_{\max}}$ and $s_{C_{\max}}$ are their associated pre-defined maximum saturation shifts. Let us mention that the Yang-Ro method also applies to tritanopes, but with other expressions for Δh and Δs .

Analysis of perceptual metrics: Color naturalness and contrast are controlled by the admissible maxima for hue (h_{\max}) and saturation values ($s_{M_{\max}}$ and $s_{C_{\max}}$). If these maxima are small, then color naturalness holds, but the contrast enhancement may be not noticeable. However, if they are not small, then there is no guarantee that the method preserves color naturalness, but image

contrast gets enhanced; for example, reddish colors may map into low-saturated blues. Nevertheless, color consistency holds, because each color always maps to a unique one.

4.3.2 HSL. In the literature, we found only one recoloring method based on HSL color space (see Reference [32]).

Iaccarino et al.'s method. As described in Reference [32], this method only applies to red-green dichromats (i.e., protanopes and deuteranopes), so the leading idea is to mitigate the confusion between reds and greens. Its pipeline is as follows: $(R, G, B) \xrightarrow{R/G\ counting} (H, S, L) \xrightarrow{\text{recoloring}} (H', S', L') \rightarrow (R', G', B')$. First, Iaccarino et al.'s method counts the number (n_R) of red-dominant pixels satisfying $R > G + 45$ and $R > B + 45$, as well as the number (n_G) of green-dominant pixels satisfying $G > R + 45$ and $G > B + 45$. If $n_R > n_G$, then the reference color is R (red); otherwise, it is G (green). Then, all pixels with non-null red or green components are recolored relative to the reference color. For pixels with colors close to the reference color, one rotates the hue 30% clockwise ($H' = (0.7H + 360) \bmod 360$), decreases the saturation 10% ($S' = 0.9S$), and increases the lightness 25% ($L' = 1.25L$); otherwise, one leaves the hue unchanged, increases the saturation 10%, and decreases the lightness 10%. Thus, the leading idea of riding off confusing reds and greens is similar to the one of Yang and Ro [92], provided that only colors close to greens or reds change their hues. The saturation and lightness variations serve the purpose of mitigating the confusion between remapped hues. Indeed, the recoloring procedure reinforces the saturation and lightness differences between hues close to reference colors (i.e., confusing colors) and those away from them, which is a sort of histogram equalization.

Analysis of perceptual metrics: Iaccarino et al.'s method enhances color contrast, because the saturation increases for some pixels and decreases for others; the same applies to lightness; also, some hues change, while others do not. In turn, color naturalness is not affected too much from the dichromat point of view, because the color components HSL are not dramatically changed. However, the method does not ensure color consistency, because the recoloring depends on the image; specifically, it depends on the dominant reference color (either red or green).

4.3.3 HSV. There are several recoloring methods using HSV color spaces, namely those in Wong and Bishop [90], Lai and Chang [43], Ching and Sabudin [12], and Ruminski et al. [74]. The latter method follows the same leading idea as the RGB-based method also introduced in Reference [74], because both take into account the CIE color distance between the original pixel color and the homologous color as seen by a red-green dichromat person. Ruminski et al. [74] also noted that red-green dichromat people only perceive two hues within the entire hue wheel, yellow 60° and blue 240°, so that they ascertained that remapping hues is useless, so only the values of saturation (S) and brightness (V) should change.

Wong-Bishop method [90]. The pipeline of this method is $(R, G, B) \rightarrow (H, S, V) \xrightarrow{\text{recoloring}} (H', S, V) \rightarrow (R', G', B')$. That is, the saturation and brightness remain unchanged so that

$$H' = H + \Delta h, \quad S' = S, \quad \text{and} \quad V' = V, \quad (6)$$

where the hue variation is given by the following non-linear mapping:

$$\Delta h = H^\theta, \quad \text{with } \theta = \theta_{\min} + \frac{n_d}{n_i + n_d} (\theta_{\max} - \theta_{\min}), \quad (7)$$

where θ stands for the control parameter of the mapping, while θ_{\min} and θ_{\max} denote its predefined minimum and maximum values within the interval $]0, 1[$; n_d and n_i represent the number of pixels falling within the distinguishable and indistinguishable hue ranges, respectively. The value of θ



Fig. 10. HSV-based recoloring method in [90]: (a) original image; (b) deutanope image view; (c) deutanope image view after recoloring. Reproduced from [90] with permission from the IEEE (©2010 IEEE).

varies from image to image. If the image hue distribution mostly falls within the indistinguishable range (i.e., reds to greens), then one increases the value of θ to stretch this range to better distinguish its hues, much like the effect of histogram equalization, as expressed by Equation (7); otherwise, if the hue distribution mostly lies outside the indistinguishable range, then one decreases θ to maintain the original hue distribution. In short, the indistinguishable hue range (i.e., reds to greens) is stretched to make confusing hues more distinguishable from each other, while the distinguishable hue range (i.e., blues) is subject to compression.

Analysis of perceptual metrics: The Wong-Bishop method also focuses on contrast enhancement in the process of remapping hues (see Reference [71] for a similar method). Furthermore, the advantage of using a power hue shift over a regular hue shift (see last methods above) is that it better preserves not only the original aesthetic feel (i.e., the loss of dynamic range in the distinguishable regions is not so noticeable) but also color naturalness. Even so, color naturalness may not hold, because sometimes hues are remapped to entirely different hues (e.g., sometimes greens are mapped to blues), as shown in Figure 10. Besides, color consistency is not preserved either, because θ changes dynamically from an image to another.

Lai-Chang method [43]. This method has the following pipeline: $(R, G, B) \xrightarrow{\text{recoloring}} (H', S, V) \xrightarrow{} (H', S, V) \xrightarrow{} (R', G', B')$. That is, it operates not only on hues but also on saturation and brightness. Nevertheless, the recoloring method depends on the color brightness. If images are neither excessively dark nor bright, then there is no need to change the color brightness, so the recoloring procedure is as follows:

$$H' = H + \Delta h, \quad S' = S + \Delta s, \quad \text{and} \quad V' = V. \quad (8)$$

But Lai and Chang do not provide any expression for Δh , because, seemingly, it depends on the visual model of each person, i.e., yellows and blues are left untouched for red-green dichromat people (i.e., protanopes and deutanopes), while reds and cyans remain unchanged for yellow-blue dichromat people (i.e., tritanopes). Also, Lai and Chang do not provide any expression for Δs .

However, if the input image is either too light or too dark, one uses histogram equalization over the brightness values of the image to reinforce its contrast as follows:

$$H' = H, \quad S' = S + \Delta s, \quad \text{and} \quad V' = V_{max} \sum_{i=0}^V \frac{n_i}{n}, \quad (9)$$

where V_{max} is the maximum possible brightness value of a given image, n_i the number of pixels with brightness i , and n the total number of pixels of such image (i.e., resolution). Note that hues remain unchanged in this case.

Analysis of perceptual metrics: The Lai-Chang method enhances the image contrast, in particular when one applies histogram equalization to too-light and too-dark images. Naturalness is preserved for too-light and too-dark images, because the hues keep their original values. However, hues suffer a rotational shift Δh in images that are neither excessively dark nor bright, which may undermine their naturalness, mainly when Δh is significant; that is, when the distance between an original color and its remapped color is two or more times the JND threshold. Color consistency does not hold, because each remapped color depends on V_{max} and n_i .

Ching-Sabudin method. As described in Reference [12], this method applies to red-green dichromats. It operates on the gamuts of reds ($H \in]300^\circ, 360^\circ[\cup [0^\circ, 60^\circ]$) and greens ($H \in]60^\circ, 180^\circ[$) separately; the blues ($H \in]180^\circ, 300^\circ[$) remain unchanged. It is also important to recall that red-green dichromats only see two hues: 60° yellow and 240° blue. Consequently, all hues in the clockwise range $] -60^\circ, 120^\circ[$ are seen as 60° , while those in the clockwise range $] 120^\circ, 300^\circ[$ are seen as 240° blue.

Then, the remapping of reds is as follows. G takes on the value of R (i.e., they are all mapped to the yellow 60°), without the need of the RGB-to-HSV conversion. In a way, this is how red-green dichromats see reds (as yellows) in natural conditions, yet with higher values of saturation and brightness as the value of G changes to the value of R .

In turn, the greens are remapped into blues to avoid confusion with reds. The confusion results from the fact that the hues of the sub-range $]60^\circ, 150^\circ[$ are also projected on the 60° yellow half-plane. In this case, one proceeds to the RGB-HSV conversion so that the recoloring takes place in the HSV color space as follows:

$$H' = H = 180 + \frac{1}{2} (H - 60), \quad S' = S, \quad \text{and} \quad V' = V, \quad (10)$$

resulting in a remapping of the hues $H \in]60^\circ, 180^\circ[$ into $]180^\circ, 240^\circ[$, so greens are mapped into blues, although it would be better to map hues from $]60^\circ, 150^\circ[$ into $]150^\circ, 240^\circ[$, because the red-green dichromat people already see hues in the sub-range $]150^\circ, 180^\circ[$ as the 240° blue.

Analysis of perceptual metrics: The Ching-Sabudin method works well for signage images, because they possess a small number of distinct regions, resulting in an apparent increase of contrast, since reds map to yellows, and greens map to blues. However, it is not suitable for real-life scenes, because the Euclidean distance between the original colors and mapped colors may be far over the JND threshold of naturalness. However, it preserves color consistency, i.e., colors always map themselves in the same manner for reds (using $G = R$) and greens (using Equation (10)).

4.4 CIE-based Methods

As noted in Section 3.4, CIE-based methods take advantage of the perceptual uniformity of the CIE color spaces. That is, the Euclidean distance between two colors is a measure of the viewer's perceptual distance. Hence, the color distance is also extensively explored in the CIE-based methods for dichromat people.

4.4.1 CIE Lab. Dichromat people perceive the values of L (brightness) and b (yellow-to-blue axis) almost correctly but not the value of a (green-to-red axis). Therefore, they do not distinguish between two colors only varying parameter is a ; hence, the color confusion of these people. There are many CIE Lab-based recoloring methods in the literature, namely: References [68], [69], [40], [84] (and its follow-ups, References [6] and [83]), as well as References [87], [35], [29] (and its follow-ups, References [88] and [89]), and also References [42] and [28] (and its follow-up, Reference [27]) and Reference [21].

Rasche et al.'s method [69]. This CIE Lab-based method is a follow-up of Reference [68] in the sense that it preserves not only the contrast between each pair of colors as in Reference [68] but also the luminance consistency. First, Rasche et al.'s method converts a given color image to its homologous grayscale image by computing the luminance $Y = 0.299 R^{2.2} + 0.587 G^{2.2} + 0.114 B^{2.2}$. However, this conversion leads to the loss of image details; that is, distinguishable details in the color image may become indistinguishable in the grayscale image. The leading idea is then to recover such image details so that the difference between any pair of colors is proportional to the difference between its homologous pair of grays. In other words, the objective is to minimize the total image error (considering all pairs colors and grays) between such differences to preserve the contrast, which is given by $\epsilon = \sum_{i=1}^{n-1} \sum_{j=i+1}^n (\|g_i - g_j\| / \|c_i - c_j\| - K)^2$, where c_i is the original pixel color, g_i is the homologous, mapped gray value, K denotes the target proportionality constant, and $\|\cdot\|$ the CIE Lab distance between colors.

The objective function (i.e., total error) of this method is thus not linear. It is a quadratic objective function that embeds contrast preservation. A possible technique to minimize such an objective function is the one known as “majorization” [14]. Furthermore, and unlike Reference [68], Rasche et al.'s method further accounts for constraints that maintain luminance consistency within narrow chrominance bands, so the modified objective function is subject to a minimization process known as *constrained majorization* [14].

Analysis of perceptual metrics: The focus of Rasche et al.'s method is on color contrast and luminance consistency, not color naturalness and color consistency. Preserving color naturalness is not achieved, because this method forces the maximization of contrast. In regards to preserving color consistency, there is no guarantee, because the color mapping depends on the specific colors existing in each image; that is, the same color in two distinct images may map to different colors.

Kovalev-Petrou method. The method in Reference [41] is a follow-up of Reference [40]. The Kovalev-Petrou method resembles Rasche et al.'s method above [68, 69], because it also uses the minimization of an objective function (i.e., error function) to preserve the color contrast of the original image (as seen by trichromat viewers) in the recolored image (as seen by dichromat viewers). However, there is no grayscale conversion as in Rasche et al.; instead, the method directly aims to preserve the perceived difference between any pair of colors of the original image and homologous pairs of colors in the recolored image. Another distinctive feature is that, in the minimization of the objective function, one only uses the 256 standard colors and their homologous dichromatic colors as follows: $\epsilon = \sum_{i=1}^n \sum_{j=1}^n w_{ij} |(\|d_i - d_j\|) - (\|c_i - c_j\|)|$, where $n = 256$ is the number of standard colors, $\|c_i - c_j\|$ and $\|d_i - d_j\|$ are Euclidean distances (in CIE Lab color space) between each pair of standard colors as seen by color-normal trichromat and dichromat people, respectively, while w_{ij} represents the frequency of the joint appearance of each pair (c_i, c_j) of colors. This frequency weight allows us to give more relevance to the colors that appear together more frequently. It is clear that any non-standard color maps itself onto its perceptually closest color of the standard palette. Finally, let us also note that the minimization of the ϵ follows a randomized approach that builds upon a greedy algorithm that iteratively changes the values of d_i and d_j .

Analysis of perceptual metrics: The Kovalev-Petrou method preserves the contrast. But, putting the focus only on preserving the contrast forces the loss of naturalness. Furthermore, color consistency does not hold, because recoloring depends on the colors existing in the input image; that is, the minimization of the error function in two distinct images may produce two distinct remapped colors for the same original color.

Wakita-Shimamura method [87]. According to Wakita and Shimamura themselves, their method does not work well for photo-images, but drawings and text (in particular, HTML text), because of

its arbitrary color replacement. In particular, it works well for HTML text recoloring consistently, yet each HTML document cannot have more than 10 colors. This method also performs the minimization of an objective function $f = C + D + N$, where $C = \sum_{i < j} w_{ij} \cdot (\|d_i - d_j\| - \|c_i - c_j\|)^2$ stands for the contrast, $D = \sum_{i < j} u_{ij} \cdot (\|d_i - d_j\| - \Delta_{\max})^2$ the color distinguishability, and $N = \sum_i v_i \cdot (\|\pi(c_i) - d_i\|)^2$ the color naturalness; in addition, $\|c_i - c_j\|$ and $\|d_i - d_j\|$ are CIE Lab distances between each pair of colors as seen in the original and remapped HTML documents, respectively, while $\pi(c_i)$ is the color c_i as perceived by a dichromat person (i.e., color projected onto the dichromat plane π); in turn, $w_{ij}, u_{ij}, v_i \geq 0$ represents the pre-defined contrast, distinguishability, and naturalness weights of each pair (c_i, c_j) of colors. Besides, Wakita and Shimura use the simulated annealing algorithm to minimize the function f .

Analysis of perceptual metrics: The Wakita-Shimamura method mainly aims to enhance the color contrast and distinguishability. Unfortunately, it may not preserve color naturalness (and color consistency), because it depends not only on the set of colors existing in each HTML document but also on those colors chosen to replace the original ones. Also, color naturalness depends on predefined weights mentioned above.

Huang et al.'s method [29] (see also its follow-ups, References [88] and [89]). Its pipeline is as follows: $(R, G, B) \rightarrow (L, a, b) \rightarrow (L, a', b') \rightarrow (R', G', B')$. Therefore, the lightness L remains unchanged. To avoid loss of detail (contrast), all except one of the points lying on the same confusion line should rotate around the convergence point in the plane ab of the CIE Lab color space. That is, one uses a rotation matrix to transform (L, a, b) into (L, a', b') , which amounts to transfer part of a in favor of b . This procedure is so because the variations of a are not perceived by red-green dichromats, which cause loss of color discrimination in the color gamut in a given image, and, consequently, loss of visual information. Regarding the CIE Lch color space, which resembles the HSV color space, this is equivalent to leave the lightness L and chroma c (saturation) untouched; only the hue changes.

The suited angle for each color is found through the minimization of an objective function $f = \varepsilon_1 + \lambda \varepsilon_2$, where $\varepsilon_1 = \sum_{i=1}^n \sum_{j=i+1}^n (\|c_i - c_j\| - \|d'_i - d'_j\|)^2$ is the error function for contrast, and $\varepsilon_2 = \sum_{i=1}^n (\|c_i - c'_i\|)^2$ is the error function for naturalness, where $c_i = (L, a, b)_i$, $c'_i = (L, a', b')_i$, and d'_i is the remapped color c'_i as seen by a dichromat person (using the Brettel et al.'s algorithm [7]); the parameter λ is a user-specified Lagrange multiplier to make a tradeoff between contrast and naturalness. The minimization of the objective function is performed through the Fletcher-Reeves conjugate-gradient method to determine the optimal solution for the rotation angle.

Analysis of perceptual metrics: According to the objective function above, Huang et al.'s method essentially tries to preserve two conflicting perceptual requirements: color contrast and color naturalness. However, if λ takes on a value less than 1, then the contrast is given more importance in detriment of naturalness. Also, color consistency does not hold, because the rotation angle varies in function of the input image.

Troiano et al.'s method [6, 83, 84]. Troiano et al.'s method was designed to help user interface designers to interactively find a suitable color palette (in the space of color palettes), and its variants; that is, a color palette that makes a good tradeoff between color accessibility and aesthetics. The leading idea is to increase the luminance contrast between contiguous colors of user interfaces, but preserving the original chromaticity of colors, as a way of guaranteeing that image details are not lost when seen by a dichromat user. Therefore, the pipeline of this method is as follows: $(R, G, B) \rightarrow (L, a, b) \rightarrow (L', a, b) \rightarrow (R', G', B')$.

The method's objective function is $f = (\prod_{i=0}^n (1 - \|c_i - c'_i\|/\Delta_{\max}) \cdot \prod_{j=1}^k r_j)^{1/(n+k)}$, where $\|c_i - c'_i\|$ is the distance between the original color c_i and its homologous mapped color c'_i , which is

normalized by maximum distance Δ_{\max} between green and blue values, r_j refers to contrast ratio between c_i and each of its k contiguous colors c_j ; the contrast ratio r_j is defined in conformity with W3C's WCAG guidelines [9]. The function f is then maximized through a genetic algorithm via the minimization of $\|c_i - c'_i\|$ and maximization of the contrast ratio between each pair of contiguous colors. Note that $f, \|c_i - c'_i\|, c_j \in [0, 1]$. The maximum value of $f = 1$ is ideal when $c_j = 1$ and $\|c_i - c'_i\| = 0$ for all (i, j) ; in practice, the value of f is below 1, because the optimization procedure varies mapped colors ($\|c_i - c'_i\| > 0$) or because some contrast ratios are below the contrast threshold ($r_j < 1$).

Analysis of perceptual metrics: In spite of only changing the lightness (L) and preserving color chromaticity, Troiano et al.'s method does not always guarantee color naturalness, because noticeable changes in lightness may change the perceived color; for example, reducing the lightness of a pink color likely gives rise to a dark red color. Besides, color consistency does not hold, because it depends not only on the colors themselves but also their adjacent colors present in a given image.

Kuhn et al.'s method. The pipeline of the method in Reference [42] is as follows: $(R, G, B) \rightarrow (L, a, b) \rightarrow (L, a', b') \rightarrow (R', G', B')$; that is, the luminance remains unchanged. In fact, red-green dichromats perceive the values of L (luminance) and b (yellow-to-blue axis) nearly in a correct manner, because the Lb plane (containing the L axis) differs from the dichromat plane in a small angle θ about the L axis; specifically, $\theta = -11.48^\circ$ for protanopes and $\theta = -8.11^\circ$ for deuteranopes. The green-to-red axis a is the color confusion axis for red-green dichromats, since all the CIE Lab colors collapse onto the dichromat plane. Therefore, they do not distinguish between two colors by only varying the value of a ; hence, the color confusion of these people. The leading idea of Kuhn et al.'s method also is to keep the distance between each pair of colors in the 2D dichromat plane equal or similar to the distance of their homologous colors in CIE Lab color space. The method consists of three steps: (i) image color quantization to get the set of key colors; (ii) optimization of the key colors in the Lb plane; and (iii) computation of the final colors in the dichromat plane from the optimized ones.

The quantization step is performed using uniform quantization or any other quantization technique (see Reference [85]), resulting in a set of key colors. The optimization step involves minimizing the difference between two distances; specifically, the distance between any pair (c_i, c_j) of key colors in the CIE Lab color space and the distance between their homologous colors (p_i, p_j) in the plane Lb . We obtain these colors in the plane Lb by the orthographic projection of (c_i, c_j) onto red-green plane color space (i.e., dichromat plane), which is then followed by rotation θ about the L axis to align it with the plane Lb . Then, the mass-spring optimization (each key color is a node of the mass-spring system) takes place in the plane Lb , where the positions of colors (p_i, p_j) are iteratively updated to find the optimized ones (p'_i, p'_j) . After that, one applies the symmetric rotation $-\theta$ from the plane Lb to dichromat plane to obtain the final colors (c'_i, c'_j) from (p'_i, p'_j) . This method also builds upon key colors, so it is necessary to carry out color interpolation to obtain a recolored image without artifacts.

Analysis of perceptual metrics: As a consequence of the optimization procedure, Kuhn et al.'s method increases the color contrast of the original image but leads to significant changes in some colors (e.g., reds sometimes map to blues), which undermines the color naturalness (cf. Figure 11). In turn, the color consistency (across a dataset of input images) is not guaranteed either, because it depends on the chromatic gamut of each image and quantization technique at hand.

Huang et al.'s method [28] (see also its follow-up, Reference [27]). Huang et al.'s pipeline is as follows: $(R, G, B) \rightarrow (L, a, b) \rightarrow (L, c, h) \rightarrow (L, c, h') \rightarrow (L, a', b') \rightarrow (R', G', B')$. The recoloring

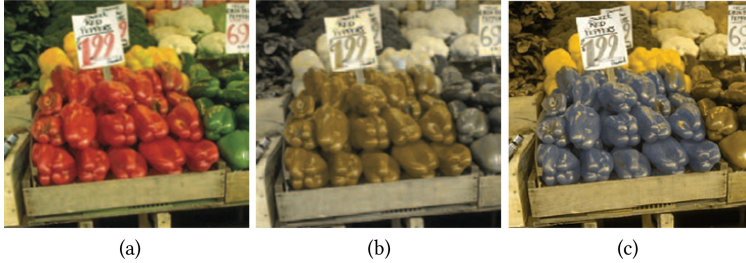


Fig. 11. CIE Lab-based recoloring method in Reference [42]: (a) original image; (b) deutanope image view; (c) deutanope image view after recoloring. Reproduced from Reference [42] with permission from the IEEE (©2008 IEEE).

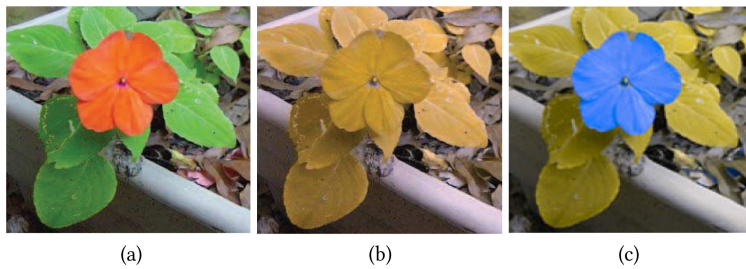


Fig. 12. CIE Lab-based recoloring method in Reference [28]: (a) original image; (b) deutanope image view; (c) deutanope image view after recoloring. Reproduced from Reference [28] with permission from the IEEE (©2009 IEEE).

mapping leaves the lightness L and chroma c (saturation) untouched. The only component that changes in the CIE Lch color space is the hue h (see Figure 12), but this induces a rotation in the plane ab of the CIE lab. Roughly speaking, the CIE Lch is similar to HSL color space, because it is also a mind color model.

Image recoloring involves four steps. First, one computes the (L, a, b) values of each pixel as its color feature. Second, pixel color features are grouped into k clusters (featuring k key colors) using the Gaussian Mixture Model (GMM), which is as a generalization of k -means clustering; the value of k determined through the minimum description length (MDL) principle [72]. Note that, Huang et al.'s method does not use color quantization to determine the key colors. Instead, k Gaussians represent the image color distribution, so avoiding image artifacts resulting from color quantization; such Gaussian functions *a priori* guarantee the smooth transition of colors between neighbor pixels. The third step carries out the optimization procedure. The idea here is to preserve, rather than to enhance, the contrast between each pair of key colors relative to trichromat color perception. For that purpose, one calculates the “distance” between each pair of Gaussians using the symmetric Kullback-Leibler (KL) divergence. Besides, Huang et al. introduced a weighting method of colors to characterize their importance for CVD people. This distance-and-weighting procedure ensures the maintenance of color contrast so that the most altered colors in the CVD condition are those ascribed with heavy weights to be able to recover the original contrast. Note that the goal is to preserve, rather than to enhance, the contrast; consequently, the centers of such those k Gaussians are re-located for a specific CVD type.

Furthermore, in the recoloring procedure, lightness (L) remains unchanged, so that the color mapping leads to rotations in the ab plane, as expressed in the pipeline above. These rotations can be represented as rotational hue shifts in the CIE Lch color space so that only the component h

changes in the optimization process. The computation of the hue shift for each color is the fourth and last step of the optimization process.

Analysis of perceptual metrics: Huang et al.'s method preserves lightness (L) in both CIE Lab and Lch color spaces and chroma (c) in the latter. Color changes occur as rotations in the plane ab of the CIE Lab color space, or, equivalently, rotations of h around the L axis of the CIE Lch color space. Therefore, this method is not effective in preserving color naturalness, because there is no control over hue shifts for confusing colors of specific CVD people. Besides, the color consistency is not ensured either, because that depends on the key colors of a given image. That is, the same color in distinct images may be mapped differently. Interestingly, Huang et al.'s method aims to preserve the contrast rather than enhancing it.

Flatla et al.'s method [21]. This color adaptation method applies to HTML documents, but there does not impede applying it to photo images. Unlike other methods, it preserves not only the perceptual experience of CVD users but also their subjective experience (i.e., subjective response). Preserving the *perceptual experience* amounts to maintain both color naturalness and contrast of a given image as much as possible. While color naturalness concerns on minimizing the CIE distance between each original color and its mapped color, color contrast is meant to maximize (or recovering) the CIE distance between each pair of mapped colors. To calculate the perceptual naturalness and contrast (differentiability), one applies the CIE76 distance, i.e., the CIE Lab Euclidean distance. With regards to the *subjective experience*, naturalness and contrast are computed using the scaled Euclidean distance concept introduced by Ou et al. [65], which measures activity, temperature, and weight; that is, this Euclidean distance is defined in the “subjective-response space.” Based on these four components (i.e., perceptual color naturalness ε_1 , perceptual color contrast ε_2 , subjective color naturalness ε_3 , and subjective color contrast ε_4), the method utilizes the objective (fitness) function $f = w_1 \varepsilon_1 + w_2 \varepsilon_2 + w_3 \varepsilon_3 + w_4 \varepsilon_4$, where the weights were determined in an empirical manner as $w_1 = w_2 = 1$ and $w_3 = w_4 = 2$, $\varepsilon_1 = (1/n) \sum_{i=1}^n \|c_i - c'_i\|$, $\varepsilon_2 = (2/(n(n-1))) \sum_{i=1}^n |(\|c_i - c_j\| - \|c'_i - c'_j\|)|$, and ε_3 (respectively, ε_4) has the same expression as ε_1 (respectively, ε_2), except that the distances are measured in the “subjective-response space”; in addition, c_i is one of the n original colors and c'_i its mapped or replacement color. This objective function is optimized using a two-pass hill-climbing algorithm.

Analysis of perceptual metrics: In conformity with its fitness function, Flatla et al.'s method preserves the contrast and naturalness as much as possible. However, as for other optimization-based methods, it does not maintain color consistency (across a dataset of images), because the mapped colors depend on the set of colors extracted from each HTML document or image.

4.4.2 CIE Luv. We have found two color adaptation methods based on CIE Luv color space for dichromat people in the literature, namely those in [60] and [53]. Milic et al.'s method was described in Section 3.4.2 (p. 9) for anomalous trichromats, but it also applies to dichromats. The only difference is that the rotation about the confusion point is more accentuated for dichromats than anomalous trichromats because of their distinct severity degrees.

Nakauchi-Onouchi method [60]. Its pipeline is as follows: $(R, G, B) \rightarrow (L, u, v) \rightarrow (L', u'v') \rightarrow (R', G', B')$, so it operates in the CIE Luv color space. This color optimization method starts with the formation of all pairs of colors in a given image, calculating then the homologous distances $\|c_i - c_j\|$ and $\|d_i - d_j\|$ in the CIE Luv for both color-normal trichromat and dichromat people, respectively. The confusing pairs of colors are those that satisfy the conditions $\|d_i - d_j\| < r\|c_i - c_j\|$ and $\|d_i - d_j\| < \|d_i - d_j\|_{\max}$, where the threshold $r = 0.9$ and $\|d_i - d_j\|_{\max} = 50.0$, though the JND is about 9.0 in CIE Luv color space.

The Nakauchi-Onouchi method consists of three main steps. First, for each pair of confusing colors, only the color with lower frequency (i.e., less number of pixels) in the image changes, and it is flagged as “changeable color.” Second, one utilizes the Linde-Buzo-Gray (LBG) algorithm [25]—a data clustering method similar to k -means—as a color clustering method that aggregates the colors of an input image into separate clusters. If more than half of colors in a specific cluster are candidates to change (i.e., “modifiable colors”), then the cluster center, and thus all its colors, must move away from the other cluster centers. Such clusters are called color-confusing clusters. Note that the cluster centers play a similar role as key colors in other methods described above. Third, the color-changing process is performed by minimizing the objective (error) function $f = \sum_{i=1}^m \delta(\mathbf{c}'_i) + \lambda \Delta(\mathbf{c}'_i)$, where m is the number of color-confusing (or modifiable) clusters, \mathbf{c}'_i is the center of the i th cluster, $\delta(\mathbf{c}'_i)$ is the confusion degree of the i th cluster, $\Delta(\mathbf{c}'_i)$ is the modification degree of the i th cluster, and $\lambda \in [0, 1]$ is a Lagrange multiplier. The confusion degree of the i th cluster is expressed as $\delta(\mathbf{c}'_i) = \sum_{j=1, j \neq i}^k \frac{1}{\|\mathbf{c}'_j - \mathbf{c}_i\| + \varepsilon}$, where k stands for the number of all color clusters, \mathbf{c}_i represents the i th cluster center, with $i = 1, \dots, k$, \mathbf{c}'_j is the center of j th color-confusing cluster, and ε is a small value to avoid divisions by zero; it is clear that $\{\mathbf{c}'_j\} \subset \{\mathbf{c}_i\}$, the set of color-confusing clusters is a subset of the set of all color clusters. In turn, the modification degree of the i th cluster is expressed as $\Delta(\mathbf{c}'_i) = \|\mathbf{c}'_i - \mathbf{c}_i\|$, where \mathbf{c}'_i is the modified cluster center of original center \mathbf{c}_i . The minimization of the objective function is performed iteratively through the gradient descent.

Analysis of perceptual metrics: The Nakauchi-Onouchi method focuses on color contrast, which is enhanced by the minimization of the objective function above. However, it does not preserve color consistency, because the objective function depends on the colors present in the input image. Color naturalness (via modification degree) may be preserved, but that depends on the Langrange multiplier λ ; specifically, it holds for values of λ close to 1.

4.4.3 CIE XYZ. To our best knowledge, there is only one recoloring method for dichromacy that builds upon the CIE XYZ color space, as described in the sequel.

Hassan-Paramesran method. The method in Reference [26] has the following pipeline: $(R, G, B) \rightarrow (X, Y, Z) \rightarrow (X', Y, Z') \rightarrow (R', G', B')$. The leading idea of this method is to perform a non-uniform rotation of the colors in the chromaticity XZ plane, so changing the color chromaticity but preserving the original luminance (i.e., the Y parameter remains unchanged).

The recoloring procedure underlying the Hassan-Paramesran method takes place in the CIE XYZ space and consists of three main steps: (i) color normalization, (ii) angular color correction, and (iii) color un-normalization. In the first step, each color c_i and its homologous dichromat color d_i (as seen by a dichromat person) are both normalized by the value of luminance Y so that the normalized luminance takes on the value 1. That is, the normalization procedure preserves the luminance of the remapped color. Let us assume that the normalized colors are denoted by $\dot{c}_i = (\dot{X}_i, \dot{Y}_i, \dot{Z}_i)$ and $\dot{d}_i = (\dot{x}_i, \dot{y}_i, \dot{z}_i)$. In the second step, one computes two error parameters $\epsilon_x = |\dot{X}_i - \dot{x}_i|$ and $\epsilon_z = |\dot{Z}_i - \dot{z}_i|$. Note that the error parameter $\epsilon_y = 0$. In addition, one computes the angles $\alpha = \tan^{-1}(\dot{Z}_i/\dot{X}_i)$ and $\beta = \tan^{-1}(\dot{z}_i/\dot{x}_i)$ of the normalized colors \dot{c}_i and \dot{d}_i in the XZ plane, respectively. The correction angle is then given by $\theta = |\alpha - \beta|$ so that the corresponding rotation matrix applies then to the vector $[\epsilon_x \ \epsilon_z]^T$ to correction vector $[\epsilon_x \ \epsilon_z]^T$. Color correction is then performed in terms of the normalized color-normal trichomat space coordinates as follows: $\dot{X}'_i = \dot{X}_i + \epsilon_x$, $\dot{Y}'_i = \dot{Y}_i$, and $\dot{Z}'_i = \dot{Z}_i + (\epsilon_x + \epsilon_z)$. Adding both ϵ_x and ϵ_z into \dot{Z}_i increases the stimulation of blues of the recolored image, and, consequently, the color perception of the red-green dichromats. Third, one performs the inverse of the first step, i.e., the un-normalization of the color $\dot{c}'_i = (\dot{X}'_i, \dot{Y}'_i, \dot{Z}'_i)$ into $c'_i = (X'_i, Y'_i, Z'_i)$, which is then converted into (R', G', B') .

Analysis of perceptual metrics: Notice that the furthest colors from the dichromat plane in the CIE XYZ color space (i.e., the vertical plane crossing the blue and yellow colors) are the most rotated, decreasing the rotation angle as the colors approach this plane. Even so, the colors do not change that much for distant colors. Therefore, the Hassan-Paramesran method preserves color naturalness as much as possible, as well as color consistency, because each color always maps in the same way.

4.5 Methods for Dichromacy: A Discussion

A brief glance at Table 2 shows the following:

- *Dichromacy types.* Most methods apply to the three types of dichromacy. But, unlike the recoloring methods for anomalous trichromat people, methods for dichromat people do not use a color compensation strategy. Instead, they use a color difference-based strategy that mitigates the red–green confusion and yellow–magenta confusion inherent to deutanope and protanope people, respectively. The compensation is not feasible, because the color space of dichromat people is not 3D but 2D. Indeed, deutanopes and protanopes only see yellows and blues, while tritanopes only see cyans and reds, with more or less brightness.
- *Color spaces.* Similarly to recoloring methods for anomalous trichromats, the CIE color spaces (14 of 29) are predominant among recoloring methods for dichromats. This fact is because CIE color spaces (except CIE XYZ) are perceptually uniform, thus suitable for color difference reinforcement. We also noted that the choice of the color space largely depends on the recoloring technique. For example, the recoloring technique based on the objective function optimization is only feasible for a limited range of colors (e.g., key colors) or when it only applies to confusing colors; otherwise, it would be a very time-consuming technique.
- *Target media.* With a few exceptions, most recoloring methods only apply to still images. As noted above, this is so because recoloring methods do not depend on the medium (e.g., a still image, an HTML document, an application interface, or even a video); they are recoloring-oriented, not medium oriented. Therefore, if a specific recoloring method works for still images, then it should also work for other media.
- *Color ranges and method types.* The color range used by a given method is closely related to the type of recoloring technique. Most methods using key colors are objective function optimization-based methods, that is, only a small set of colors of the input image are directly subject to the recoloring; one obtains the remaining remapped colors by interpolation. In turn, matrix-based methods are pixelwise in the sense their recoloring procedure directly applies to each image pixel, that is, multiplying the recoloring matrix by an input color, one obtains the homologous remapped color. Furthermore, Table 2 shows that most optimization-based methods take advantage of CIE color spaces, as they use objective functions to iteratively increase distances between confusing colors and enhance the contrast. In regards to matrix-based methods, they use matrices of linear and non-linear transformations (i.e., rotation matrix, shrinking matrix, and so forth) to remap the original colors of a given image into more contrasting colors. For example, most HSx-based methods (see, for instance, References [32, 92]) use a rotation matrix to color remapping, while some RGB-based techniques (see, for example, Reference [2]) decrease one or two color components to increase the remaining color components.
- *Perceptual requirements.* As for anomalous trichromats, the methods for dichromats focus on preserving or enhancing color contrast, and this is particularly important to distinguish between confusing colors in their 2D color space. Recall that confusion mainly results from the amalgamation of the 3D color space of the input image onto the 2D color space of dichromat

Table 2. Recoloring Methods for Dichromat People

Reference	Dichromacy			Color space	Target media				Color range	Method type	Perceptual metrics			
	P	D	T		I	D	H	M			M	O	CE	CC
Yang and Ro [92]	•	•	•	HSI	•				TC	•		•	•	
Kovalev [40]	•	•	•	Lab	•				key		•	•		
Kovalev and Petrou [41]	•	•		Lab	•				key		•	•		
Wakita and Shimamura [87]	•	•	•	Lab		•	•		key		•	•		
Rasche et al. [68]	•	•	•	Lab	•				key		•	•		
Rasche et al. [69]	•	•	•	Lab	•				key		•	•		
Iaccarino et al. [32]	•	•		HSL	•				TC	•		•	•	
Jefferson and Harvey [35]	•	•	•	RGB	•				key		•	•		
Jefferson and Harvey [36]	•	•	•	LMS	•				TC	•		•	•	
Huang et al. [29]	•	•		Lab	•				TC		•	•		
Anagnostopoulos et al. [1]	•			RGB	•				TC	•		•	•	
Deng et al. [16]	•	•	•	RGB	•				key		•	•	•	
Bao et al. [2]	•	•	•	RGB	•				TC	•		•	•	
Kuhn et al. [42]	•	•	•	Lab	•				key		•	•		
Nakauchi and Onouchi [60]	•	•	•	Luv	•	•			key		•	•		
Ma et al. [49]	•	•	•	RGB	•				key		•	•		
Troiano et al. [84]	•	•	•	Lab		•			TC		•	•		
Wong and Bishop [90]	•	•	•	HSV	•				TC	•		•		
Doliotis et al. [17]	•			RGB	•				TC	•		•	•	
Wang et al. [88]	•	•		Lab	•				key		•	•		
Lai and Chang [43]	•	•	•	HSV	•				TC	•		•		
Huang et al. [28]	•	•	•	Lab	•				key		•	•		
Huang et al. [27]	•	•	•	Lab	•				key		•	•		
Ruminski et al. [74]	•	•	•	RGB	•				TC	•		•	•	
Ruminski et al. [74]	•	•	•	HSV	•				TC	•		•	•	
Ching and Sabudin [12]	•	•		HSV	•	•			TC	•		•	•	
Chen et al. [10]	•	•		LMS			•		key	•		•	•	
Flatla et al. [21]	•	•	•	Lab		•			key		•	•	•	
Hassan and Paramesran [26]	•	•		XYZ	•				TC	•		•	•	

Abbreviations:

Dichromacy: P (protanopia); D (deutanopia); T (tritanopia).

Target media: I (still images); D (drawings, charts, and signage); H (HTML documents); M (medical imaging).

Color range: TC (true color); key (key colors, key color look-up table, or just a few colors).

Method type: M (matrix-based); O (optimization-based).

Perceptual metrics: CC (color consistency); CE (contrast enhancement); NP (naturalness preservation).

people. Most of these methods are not color-consistent and are not able to preserve color naturalness either. Moreover, no method satisfies the three perceptual requirements simultaneously. Therefore, no method preserves the perceptual learning of dichromat people.

Thus, the main conclusions we can draw from the state-of-the-art methods for anomalous trichromats are the following:

- It is not feasible to make dichromats see as color-normal trichromats simply because dichromat only see two hues, with more or less saturation and brightness; for example, red-green

dichromats only perceive two hues, 60° yellow and 240° blue. All the other colors collapse on the dichromat plane defined by 60° yellow and 240° blue. Thus, and unlike we observed for anomalous trichromats, the evaluation naturalness has to be performed from the dichromat's point of view, not from the color-normal trichromat's standpoint.

- In respect to preserve the perceptual learning of dichromat people as much as possible, optimization-based methods seemingly are better than matrix-based methods, because error functions for contrast and naturalness can be incorporated into an objective function. However, color contrast and naturalness are conflicting metrics. Consequently, a minimum of the objective function only guarantees a tradeoff between contrast and naturalness. Nevertheless, in some circumstances, as it is the case of signage and medicine imaging, naturalness is much less important than contrast for the perception of dichromats; for example, increasing the contrast is essential to make distinguishable two objects in an image that are indistinguishable otherwise.
- Taking into consideration that every 3D color space collapses onto a 2D color space under dichromacy conditions, it is quite difficult to devise a content-dependent recoloring method for dichromats. This so because the number of non-confusing colors of an image is potentially small when seen by a dichromat person.

In general, optimization-based recoloring methods work better than matrix-based methods for dichromats, because one quickly finds a tradeoff between contrast and naturalness. The question then is which is the best objective function that combines contrast and naturalness, since there is no way of making a dichromat see as a color-normal trichromat person.

5 CVD RECOLORING METHODS FOR MONOCHROMACY

Monochromats see colors in grayscale and sometimes with slight shades of blue. That is, the color space of monochromat people is one dimensional. Thus, monochromacy significantly reduces the ability of discriminating objects in images, mainly when they have the same perceptual luminance. That is, two objects with the same luminance are only distinguishable if we change at least the luminance of one of them.

5.1 CIE-based Methods

5.1.1 CIE Lab. In the literature, there are only a couple of methods for recoloring still images for monochromat people, specifically those in References [68] and [69], which are both based on CIE Lab color space.

Rasche et al.'s method [68]. Rasche et al.'s method works for both monochromat and dichromat people. Besides, it takes advantage of the same error function used in Reference [68] for dichromacy (see Section 4.4.1), which takes the form $\varepsilon^2 = \sum_{i=1}^n \sum_{j=i+1}^n \left(\frac{\|c_i - c_j\|}{D_{max}} - \frac{|g \cdot (c_i - c_j)|}{d_{max}} \right)^2$ for monochromacy, where g stands for the luminance, whose initial value is $(1, 0, 0)$, being its optimal value determined by minimizing the error ε through the Fletcher-Reeves conjugate-gradient method. Recall that the goal is to preserve the contrast between each pair of colors, c_i and c_j . D_{max} is the maximum distance between any pair of colors in the CIE Lab color space, while d_{max} is the maximum distance between any pair of colors in the 2D dichromat plane.

Analysis of perceptual metrics: Given any pair of colors, Rasche et al.'s method assumes that the perceived color difference between them should be proportional to their corresponding, perceived gray difference (see Figure 13). This assumption translates into the minimization of the error function above to guarantee the confusing colors get distinct luminance values. Consequently, both color naturalness and consistency do not hold.

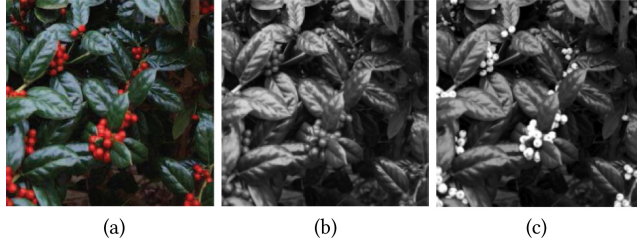


Fig. 13. CIE Lab-based recoloring method in Reference [68]: (a) original image; (b) deutan image view; (c) deutan image view after recoloring with $g = (1, 0, 0)$. Reproduced from Reference [68] with permission from the IEEE (©2005 IEEE).

Table 3. Summary of the Color Adaptation Methods for Monochromacy

Reference	Monochromacy		Color space	Target medium		Color range	Perceptual metrics		
	blue-cone	rod		I	D		CE	CC	NP
Rasche et al. [68]	•	•	Lab	•	•	key	•		
Rasche et al. [69]	•	•	Lab	•	•	key	•		

Abbreviations:

Monochromacy types: blue-cone; rod.

Target medium: I (still images); D (drawings, charts, and signage).

Color range: key (key colors).

Properties: CE (contrast enhancement); CC (color consistency); NP (naturalness preservation).

Rasche et al.’s method [69]. The method described in Reference [69] is a follow-up of the method in Reference [68]. This follow-up is also valid for both monochromat and dichromat people. However, it uses a different objective function $\varepsilon = \sum_{i=1}^{n-1} \sum_{j=i+1}^n (\|g_i - g_j\| / \|c_i - c_j\| - K)^2$, where c_i and c_j are original pixel colors, g_i and g_j are the homologous, mapped gray value, K denotes the target proportionality constant, and $\|\cdot\|$ the CIE Lab distance between colors. Note that the mapped colors are in grayscale so that the leading idea is to preserve both contrast and luminance consistency. These two goals are formulated as a constrained, multi-dimensional scaling problem [14]. As in Reference [68], one preserves contrast by keeping the relative distance between each pair of colors in the recoloring process. Then, one adds constraints that reinforce luminance consistency so that one describes the desired solution as a sequence of linear programming problems.

Analysis of perceptual metrics: As expected, and similarly to Reference [68], the present method preserves neither color naturalness nor color consistency, because its focus is only on preserving image contrast in the grayscale.

5.2 Methods for Monochromacy: A Discussion

As shown in Table 3, there are only two methods developed for monochromat people, both built upon CIE Lab color space. These two methods take advantage of objective function optimization; hence, the small range of key colors. Consequently, they are neither color consistent nor natural compliant. That is, the focus of such methods is on ensuring the contrast between confusing colors.

6 CRITICAL ANALYSIS AND TRENDS FOR THE FUTURE

Given the recoloring methods above, only those designed for trichromat people preserve the perceptual learning of CVD people, because, in general, they satisfy the perceptual requirements of color contrast, color consistency, and color naturalness simultaneously. However, these recoloring

methods work in a pixelwise manner, without considering any semantics about the contents of the input image. In a way, we are using blind methods for colorblind people. Indeed, often image regions featuring objects do not need to be subject to recoloring at all. Note that the pixelwise nature of most recoloring methods makes contrast and naturalness conflicting requirements.

To solve this paradox in the future, we need to incorporate semantics into recoloring methods. In the literature, there already are some trends that point to this direction of semantic recoloring methods. Among them, we find the following:

- *Pattern pinning.* A way of mitigating or even eliminating confusion in the perception of color is pinning text or geometric patterns to pixels. See, for example, References [76] and [19] for further details. The disadvantage of this technique is that it provokes visual noise to CVD people.
- *Selective contour enhancement.* A couple of methods are already capable of selecting color-confusing objects in a given image, enhancing then their contours without changing their interiors (e.g., see References [81] and [3] for further details). The advantage of this technique is the improvement of the contrast (e.g., using image filters) without penalizing color consistency and naturalness.
- *Selective addition of visual effects.* An alternative way of discriminating objects seen with the same color is the selective representation of the repetitions with visual effects, giving to it a sensation of 3D. Chua et al.’s method [13] takes advantage of the Luster Effect to achieve that, in a natural way and by preserving color consistency.

Let us also mention that there is also an unexplored research direction that has to do with the semantic extraction of objects from images to identify those that need to be subject to color adaptation. In other words, we need to move from the pixelwise to the objectwise paradigm. The advances in the *concept detection* area (see, for example, Huiskes et al. [31]) and other areas related to the extraction of semantic from images are quite promising in the CVD adaptation.

7 CONCLUSIONS

In the past two decades, a significant number of recoloring algorithms for CVD people have been proposed in the literature, mostly focused on still images, although there are also works whose target is another type of medium (e.g., text, video, HTML documents, and so forth).

We have shown that recoloring methods must satisfy three perceptual requirements (i.e., contrast enhancement, color consistency, and color naturalness) in order not to disturb that much the perceptual learning of CVD people. Indeed, preserving perceptual learning is the most important requirement to take into consideration when designing a new recoloring method. In our opinion, this is the most important contribution of the study carried out in this survey.

ACKNOWLEDGMENTS

We are grateful to the reviewers for their criticism that helped us to significantly improve this article.

REFERENCES

- [1] C.-N. Anagnostopoulos, G. Tsekouras, I. Anagnostopoulos, and C. Kalloniatis. 2007. Intelligent modification for the daltonization process of digitized paintings. In *Proceedings of the 5th International Conference on Computer Vision Systems (ICVS’07)*.
- [2] J. Bao, Y. Wang, Y. Ma, and X. Gu. 2008. Re-coloring images for dichromats based on an improved adaptive mapping algorithm. In *Proceedings of the International Conference on Audio, Language and Image Processing (ICALIP’08)*. IEEE Press, 152–156.

- [3] S. Bao, G. Tanaka, H. Tamukoh, and N. Suetake. 2016. Lightness modification method considering Craik-O'Brien effect for protanopia and deutanopia. *IEICE Trans. Fundam. Electr. Commun. Comput. Sci.* E99. A, 11 (2016), 2008–2011.
- [4] J. Birch. 2001. *Diagnosis of Defective Colour Vision* (2nd ed.). Elsevier Science, Edinburgh.
- [5] J. Birch, I. Chisholm, P. Kinnear, M. Marré, A. Pinckers, J. Pokorny, and G. Verriest. 1979. Acquired color vision defects. In *Congenital and Acquired Color Vision Defects*. Grune & Stratton.
- [6] C. Birtolo, P. Pagano, and L. Troiano. 2009. Evolving colors in user interfaces by interactive genetic algorithm. In *Proceedings of the World Congress on Nature and Biologically Inspired Computing (NaBIC'09)*. IEEE Computer Society, 349–355.
- [7] H. Bretell, F. Viénot, and J. Mollon. 1997. Computerized simulation of color appearance for dichromats. *J. Opt. Soc. Am.* 14, 10 (1997), 2647–2655.
- [8] A. Byrne and D. Hilbert. 2010. How do things look to the color-blind? In *Color Ontology and Color Science*, J. Cohen and M. Metthen (Eds.). MIT Press.
- [9] B. Caldwell, M. Cooper, L. Reid, and G. Vanderheiden. 2008. Web content accessibility guidelines (WCAG) 2.0. The World Wide Web Consortium. Retrieved from <https://www.w3.org/TR/WCAG20>.
- [10] W. Chen, W. Chen, and H. Bao. 2011. An efficient direct volume rendering approach for dichromats. *IEEE Trans. Vis. Comput. Graph.* 17, 12 (2011), 2144–2152.
- [11] Y.-C. Chen and T.-S. Liao. 2011. Hardware digital color enhancement for color vision deficiencies. *ETRI J.* 33, 1 (2011), 71–77.
- [12] S.-L. Ching and M. Sabudin. 2010. Website image colour transformation for the colour blind. In *Proceedings of the 2nd International Conference on Computer Technology and Development (ICCTD'10)*. IEEE Computer Society, 255–259.
- [13] S. H. Chua, H. Zhang, M. Hammad, S. Zhao, S. Goyal, and K. Singh. 2015. ColorBless: Augmenting visual information for colorblind people with binocular luster effect. *ACM Trans. Comput.-Hum. Interact.* 21, 6 (2015), A32:1–A32:20.
- [14] T. Cox and M. Cox. 2001. *Multidimensional Scaling* (2nd ed.). Chapman & Hall/CRC, Boca Raton, FL, USA.
- [15] A. Damasio, T. Yamada, H. Damasio, J. Corbett, and J. McKee. 1980. Central achromatopsia: behavioral, anatomic, and physiologic aspects. *Neurology* 30, 10 (1980), 1064–1071.
- [16] Y. Deng, Y. Wang, Y. Ma, J. Bao, and X. Gu. 2007. A fixed transformation of color images for dichromats based on similarity matrices. In *Proceedings of the 3rd International Conference on Intelligent Computing (ICIC'07)*, Lecture Notes in Computer Science, Vol. 4681. Springer, Berlin, 1018–1028.
- [17] P. Doliotis, G. Tsekouras, C.-N. Anagnostopoulos, and V. Athitsos. 2009. Intelligent modification of colors in digitized paintings for enhancing the visual perception of color-blind viewers. In *Proceedings of the IFIP International Conference on Artificial Intelligence Applications and Innovations (AIAI'09)*, Vol. 296. Springer, Berlin, 293–301.
- [18] M. Fairchild. 2013. *Color Appearance Models* (3rd ed.). John Wiley & Sons, Ltd.
- [19] D. Flatla, A. Andrade, R. Teviotdale, D. Knowles, and C. Stewart. 2015. ColourID: Improving colour identification for people with impaired colour vision. In *Proceedings of the 33rd Annual ACM Conference on Human Factors in Computing Systems (CHI'15)*. ACM Press, 3543–3552.
- [20] D. Flatla and C. Gutwin. 2012. SSMRecolor: Improving recoloring tools with situation-specific models of color differentiation. In *Proceedings of the 30th International Conference on Human factors in Computing Systems (CHI'12)*. ACM Press, 2297–2306.
- [21] D. Flatla, K. Reinecke, C. Gutwin, and K. Gajos. 2013. SPRWeb: Preserving subjective responses to website colour schemes through automatic recolouring. In *Proceedings of the Conference on Human Factors in Computing Systems (CHI'2013)*. ACM Press, 2069–2078.
- [22] B. Fraser, C. Murphy, and F. Bunting. 2005. *Real World Color Management* (2nd ed.). Peachpit Press, Berkeley, CA.
- [23] J. Gardner, M. Michaelides, G. Holder, N. Kanuga, T. Webb, J. Mollon, A. Moore, and A. Hardcastle. 2009. Blue cone monochromacy: Causative mutations and associated phenotypes. *Molec. Vis.* 15 (2009), 876–884.
- [24] R. Gonzalez and R. Woods. 1992. *Digital Image Processing*. Pearson, Prentice Hall.
- [25] R. Gray, J. Kieffer, and Y. Linde. 1980. Locally optimal block quantizer design. *Inf. Contr.* 45, 2 (1980), 178–198.
- [26] M. Hassan and R. Paramesran. 2017. Naturalness preserving image recoloring method for people with red-green deficiency. *Sign. Process.: Image Commun.* 57 (2017), 126–133.
- [27] C.-R. Huang, K.-C. Chiu, and C.-S. Chen. 2010. Key color priority based image recoloring for dichromats. In *Proceedings of the 11th Pacific-Rim Conference on Multimedia (PCM'10)*, Lecture Notes in Computer Science, Vol. 6298. Springer-Verlag, Berlin, 637–647.
- [28] J.-B. Huang, C.-S. Chen, T.-C. Jen, and S.-J. Wang. 2009. Image recolorization for the colorblind. In *Proceedings of the International Conference on Acoustics, Speech, and Signal Processing (ICASSP'09)*. IEEE Press, 1161–1164.
- [29] J.-B. Huang, Y.-C. Tseng, S.-I. Wu, and S.-J. Wang. 2007. Information preserving color transformation for protanopia and deutanopia. *Sign. Process. Lett.* 14, 10 (2007), 711–714.

- [30] J.-B. Huang, S.-Y. Wu, and C.-S. Chen. 2008. Enhancing color representation for the color vision impaired. In *Proceedings of the Workshop on Enhancing Color Representation for the Color Vision Impaired, Held in Conjunction with the 10th European Conference on Computer Vision (ECCV'08)*.
- [31] M. Huiskes, B. Thomee, and M. Lew. 2010. New trends and ideas in visual concept detection: The MIR flickr retrieval evaluation initiative. In *Proceedings of the 11th ACM International Conference on Multimedia Information Retrieval (MIR'10)*. ACM Press, 527–536.
- [32] G. Iaccarino, D. Malandrino, M. Del Percio, and V. Scarano. 2006. Efficient edge-services for colorblind users. In *Proceedings of the 15th International Conference on World Wide Web (WWW'06)*. ACM Press, 919–920.
- [33] M. Ichikawa, K. Tanaka, S. Kondo, K. Hiroshima, K. Ichikawa, S. Tanabe, and K. Fukami. 2003. Web-page color modification for barrier-free color vision with genetic algorithm. In *Proceedings of the Genetic and Evolutionary Computation Conference (GECCO'03)*, Lecture Notes in Computer Science, Vol. 2724. Springer, Berlin, 2134–2146.
- [34] M. Ichikawa, K. Tanaka, S. Kondo, K. Hiroshima, K. Ichikawa, S. Tanabe, and K. Fukami. 2004. Preliminary study on color modification for still images to realize barrier-free color vision. In *Proceedings of the IEEE International Conference on Systems, Man and Cybernetics*, Vol. 1. IEEE Press, 36–41.
- [35] L. Jefferson and R. Harvey. 2006. Accommodating color blind computer users. In *Proceedings of the 8th International ACM SIGACCESS Conference on Computers and Accessibility (ASSETS'06)*. ACM Press, 40–47.
- [36] L. Jefferson and R. Harvey. 2007. An interface to support color blind computer users. In *Proceedings of the Conference on Human Factors in Computing Systems (CHI'2007)*. ACM Press, 1535–1538.
- [37] J.-Y. Jeong, H.-J. Kim, T.-S. Wang, Y.-J. Yoon, and S.-J. Ko. 2011. An efficient re-coloring method with information preserving for the color-blind. *IEEE Trans. Cons. Electr.* 57, 4 (2011), 1953–1960.
- [38] T. Kojima, R. Mochizuki, R. Lenz, and J. Chao. 2014. Riemann geometric color-weak compensation for individual observers. In *Proceedings of the Universal Access in Human-Computer Interaction (UAHCI'14)*, Lecture Notes in Computer Science, Vol. 8514. Springer, Cham, Switzerland, 121–131.
- [39] H. Kolb, E. Fernandez, and R. Nelson (Eds.). 2011. *WebVision: The Organization of the Retina and Visual System*. John Moran Eye Center, University of Utah, Salt Lake City, UT. Retrieved from <http://webvision.med.utah.edu/>.
- [40] V. Kovalev. 2004. Towards image retrieval for eight percent of color-blind men. In *Proceedings of the 17th International Conference on Pattern Recognition (ICPR'04)*, Vol. 2. IEEE Press, 943–946.
- [41] V. Kovalev and M. Petrou. 2005. Optimising the choice of colours of an image database for dichromats. In *Proceedings of the 4th International Conference on Machine Learning and Data Mining in Pattern Recognition (MLDM'05)*, Lecture Notes in Computer Science, Vol. 3587. Springer, Berlin, 456–465.
- [42] G. Kuhn, M. Oliveira, and L. Fernandes. 2008. An efficient naturalness-preserving image-recoloring method for dichromats. *IEEE Trans. Vis. Comput. Graph.* 14, 6 (2008), 1747–1754.
- [43] C.-L. Lai and S.-W. Chang. 2009. An image processing based visual compensation system for vision defects. In *Proceedings of the 5th International Conference on Intelligent Information Hiding and Multimedia Signal Processing (IIH-MSP'09)*. IEEE Computer Society, 559–562.
- [44] J. Lee and W. Santos. 2010. An adaptative fuzzy-based system to evaluate color blindness. In *Proceedings of the 17th International Conference on Systems, Signals and Image Processing (IWSSIP'10)*. 211–214.
- [45] J. Lee and W. Santos. 2011. An adaptive fuzzy-based system to simulate, quantify and compensate color blindness. *Integr. Comput.-Aid. Eng.* 18, 1 (2011), 29–40.
- [46] M. Luo, G. Cui, and C. Li. 2006. Uniform colour spaces based on CIECAM02 colour appearance model. *Color Res. Appl.* 31, 4 (2006), 320–330.
- [47] M. R. Luo and R. W. G. Hunt. 1998. The structure of the CIE 1997 colour appearance model (CIECAM97s). *Color Res. Appl.* 23, 3 (1998), 138–146.
- [48] Y. Ma, X. Gu, and Y. Wang. 2006. A new color blindness cure model based on bp neural network. In *Proceedings of the 3rd International Symposium on Neural Networks (ISNN'06)*, Lecture Notes in Computer Science, Vol. 3973. Springer-Verlag, Berlin, 740–745.
- [49] Y. Ma, X. Gu, and Y. Wang. 2008. Color discrimination enhancement for dichromats using self-organizing color transformation. *Inf. Sci.* 179, 6 (2008), 830–843.
- [50] G. Machado. 2010. *A Model for Simulation of Color Vision Deficiency and a Color Contrast Enhancement for Dichromats*. Ph.D. Dissertation. Universidade Federal do Rio Grande do Sul, Porto Alegre, Brazil.
- [51] G. M. Machado, M. M. Oliveira, and L. Fernandes. 2009. A physiologically-based model for simulation of color vision deficiency. *IEEE Trans. Vis. Comput. Graph.* 15, 6 (2009), 1291–1298.
- [52] E. Marieb and K. Hoehn. 2010. *Human Anatomy & Physiology* (8th ed.). Benjamin-Cummings Publishing Company, San Francisco, CA.
- [53] N. Milic, M. Hoffmann, T. Tomacs, D. Novakovic, and B. Milosavljevic. 2015. A content-dependent naturalness-preserving daltonization method for dichromatic and anomalous trichromatic color vision deficiencies. *J. Imag. Sci. Technol.* 59, 1 (2015), 010504.
- [54] Y. Miyake. 2006. *Electrodiagnosis of Retinal Diseases*. Springer-Verlag, Tokyo, Japan.

- [55] R. Mochizuki, T. Nakamura, J. Chao, and R. Lenz. 2008. Color-weak correction by discrimination threshold matching. In *Proceedings of the 5th Conference on Colour in Graphics, Imaging and Vision (CGIV'08)*. Society for Imaging Science and Technology, 208–213.
- [56] R. Mochizuki, S. Oshima, and J. Chao. 2011a. Fast color-weakness compensation with discrimination threshold matching. In *Proceedings of the 3rd International Workshop on Computational Color Imaging (CCIW'11)*, Lecture Notes in Computer Science, Vol. 6626. Springer, Berlin, 176–187.
- [57] R. Mochizuki, S. Oshima, R. Lenz, and J. Chao. 2011b. Exact compensation of color-weakness with discrimination threshold matching. In *Proceedings of the 6th International Conference on Universal Access in Human-Computer Interaction (UAHCI'11)*, Lecture Notes in Computer Science, Vol. 6768. Springer, Berlin, 155–164.
- [58] J. Mollon, F. Newcombe, P. Polden, and G. Ratcliff. 1980. On the presence of three cone mechanisms in a case of total achromatopsia. In *Proceedings of the 5th Symposium of the International Research Group on Colour Vision Deficiencies*, G. Verriest (Ed.). Adam Hilger, Bristol, United Kingdom, 130–135.
- [59] J. Morovic and M. Luo. 1999. Developing algorithms for universal colour gamut mapping. In *Colour Imaging: Vision and Technology*, L. MacDonald and M. Luo (Eds.). John Wiley & Sons Ltd., 253–283.
- [60] S. Nakuchi and T. Onouchi. 2008. Detection and modification of confusing color combinations for red-green dichromats to achieve a color universal design. *Color Res. Appl.* 33, 3 (2008), 203–211.
- [61] Jamie R. Nuñez, Christopher R. Anderton, and Ryan S. Renslow. 2018. Optimizing colormaps with consideration for color vision deficiency to enable accurate interpretation of scientific data. *PLoS One* 13, 7 (2018), e0199239:1–14.
- [62] S. Oshima, R. Mochizuki, J. Chao, and R. Lenz. 2009. Color reproduction using riemann normal coordinates. In *Proceedings of the 2nd International Computational Color Imaging Workshop (CCIW'09)*, Lecture Notes in Computer Science, Vol. 5646. Springer, Berlin, 140–149.
- [63] S. Oshima, R. Mochizuki, R. Lenz, and J. Chao. 2012. Color-weakness compensation using riemann normal coordinates. In *Proceedings of the 2012 IEEE International Symposium on Multimedia (ISM'12)*. IEEE Computer Society, 175–178.
- [64] S. Oshima, R. Mochizuki, R. Lenz, and J. Chao. 2016. Modeling, measuring, and compensating color weak vision. *IEEE Trans. Image Process.* 25, 6 (2016), 2587–2600.
- [65] L.-C. Ou, M. Luo, A. Woodcock, and A. Wright. 2004. A study of colour emotion and colour preference. Part I: Colour emotions for single colours. *Color Res. Appl.* 29, 3 (2004), 232–240.
- [66] L. Petrich. 2012. Color-Blindness Simulators. Retrieved October 28, 2017 from <http://lpetrich.org/Science/ColorBlindnessSim/ColorBlindnessSim.html>.
- [67] S. Poret, R. Dony, and S. Gregori. 2009. Image processing for colour blindness correction. In *Proceedings of the International Conference on Science and Technology for Humanity (TIC-STH'09)*. IEEE Computer Society, 539–544.
- [68] K. Rasche, R. Geist, and J. Westall. 2005a. Detail preserving reproduction of color images for monochromats and dichromats. *IEEE Comput. Graph. Appl.* 25, 3 (2005), 22–30.
- [69] K. Rasche, R. Geist, and J. Westall. 2005b. Re-coloring images for gamuts of lower dimension. *Comput. Graph. Forum* 24, 3 (2005), 423–432.
- [70] A. Reitner, L. Sharpe, and E. Zrenner. 1991. Is colour vision possible with only rods and blue-sensitive cones? *Nature* 352, 6338 (1991), 798–800.
- [71] M. Ribeiro and A. Gomes. 2013. A skillet-based recoloring algorithm for dichromats. In *Proceedings of the 15th International Conference on e-Health Networking, Applications and Services (Healthcom'2013)*. IEEE Computer Society, 654–658.
- [72] J. Rissanen. 1997. Stochastic complexity in learning. *J. Comput. Syst. Sci.* 55, 1 (1997), 89–95.
- [73] R.-L. Rousseau. 1980. *Le Language Des Couleurs*. Éditions Dangles, St. Jean de Braye, France.
- [74] J. Ruminski, J. Wtorek, J. Ruminska, M. Kaczmarek, A. Bujnowski, T. Kocejko, and A. Polinski. 2010. Color transformation methods for dichromats. In *Proceedings of the 3rd Conference on Human System Interactions (HSI'10)*. IEEE Computer Society, 634–641.
- [75] L. Ruttinger, D. Braun, K. Gegenfurtner, D. Petersen, P. Schonle, and L. Sharpe. 1999. Selective color constancy deficits after circumscribed unilateral brain lesions. *J. Neurosci.* 9, 8 (1999), 3094–3106.
- [76] B. Sajadi, A. Majumder, M. Oliveira, R. Schneider, and R. Raskar. 2013. Using patterns to encode color information for dichromats. *IEEE Trans. Vis. Comput. Graph.* 19, 1 (2013), 118–129.
- [77] J. Sammon. 1969. A nonlinear mapping for data structure analysis. *IEEE Trans. Comput.* 18, 5 (1969), 401–409.
- [78] L. Sharpe, A. Stockman, H. Jägle, and J. Nathans. 1999. Opsin genes, cone photopigments, color vision and color blindness. In *Color Vision: From Genes to Perception*, K. Gegenfurtner and L. Sharpe (Eds.). Cambridge University Press.
- [79] Prarthana Shrestha and Bas Hulskens. 2014. Color accuracy and reproducibility in whole slide imaging scanners. *J. Med. Imag.* 1, 2 (2014), 027501:1–8.
- [80] N. Smith. 2017. Colors spacious documentation 2017. Retrieved from <https://colorspacious.readthedocs.org/en/latest>.

- [81] N. Suetake, G. Tanaka, H. Hashii, and E. Uchino. 2012. Simple lightness modification for color vision impaired based on Craik-O'Brien effect. *J. Frank. Inst.* 349, 6 (2012), 2093–2107.
- [82] M. Tkalcic and J. Tasic. 2003. Colour spaces: Perceptual, historical and applicational background. In *Proceedings of the IEEE Region 8 International Conference on Computer as a Tool (EUROCON'03)*. IEEE Computer Society, 304–308.
- [83] L. Troiano, C. Birtolo, and G. Cirillo. 2009. Interactive genetic algorithm for choosing suitable colors in user interface. In *Proceedings of 3rd International Conference on Learning and Intelligent Optimization (LION'09)*.
- [84] L. Troiano, C. Birtolo, and M. Miranda. 2008. Adapting palettes to color vision deficiencies by genetic algorithm. In *Proceedings of the 10th Annual Conference on Genetic and Evolutionary Computation (GECCO'08)*. ACM Press, 1065–1072.
- [85] L. Velho, A. Frery, and J. Gomes. 2008. *Image Processing for Computer Graphics and Vision*. Springer-Verlag, London.
- [86] F. Vienot, H. Brettel, and J. Mollon. 1999. Digital video colourmaps for checking the legibility of displays by dichromats. *Color Res. Appl.* 24, 4 (1999), 243–252.
- [87] K. Wakita and K. Shimamura. 2005. SmartColor: Disambiguation framework for the colorblind. In *Proceedings of the 19th International ACM SIGACCESS Conference on Computers and Accessibility (ASSETS'05)*. ACM Press, 158–165.
- [88] M. Wang, B. Liu, and X. Hua. 2009. Accessible image search. In *Proceedings of the 17th ACM International Conference on Multimedia (MM'09)*. ACM Press, 291–300.
- [89] M. Wang, B. Liu, and X. Hua. 2010. Accessible image search for colorblindness. *ACM Trans. Intell. Syst. Technol.* 1, 1, Article 8 (2010), 1–26.
- [90] A. Wong and W. Bishop. 2008. Perceptually-adaptive color enhancement of still images for individuals with dichromacy. In *Proceedings of the Canadian Conference on Electrical and Computer Engineering (CCECE'08)*. IEEE Computer Society, 2027–2032.
- [91] S. Woo, C. Park, Y. S. Baek, and Y. Kwak. 2018. Flexible technique to enhance color-image quality for color-deficient observers. *Curr. Opt. Photon.* 2, 1 (2018), 101–106.
- [92] S. Yang and Y. Ro. 2003. Visual contents adaptation for color vision deficiency. In *Proceedings of the 2003 International Conference on Image Processing (ICIP'03)*, Vol. 1. IEEE Computer Society, 453–456.
- [93] S. Yang, Y. Ro, J. Nam, J. Hong, S. Choi, and J. Lee. 2004. Improving visual accessibility for color vision deficiency based on MPEG-21. *ETRI J.* 26, 3 (2004), 195–202.
- [94] S. Yang, Y. Ro, E. Wong, and J. Lee. 2008. Quantification and standardized description of color vision deficiency caused by anomalous trichromats – part I: Simulation and measurement. *EURASIP J. Image Vid. Process.* 2008 (2008), Article 487618, 9.
- [95] J. You and K.-C. Park. 2016. Image processing with color compensation using LCD display for color vision deficiency. *J. Display Technol.* 12, 6 (2016), 562–566.

Received October 2017; revised December 2018; accepted April 2019